



TECHNISCHE
UNIVERSITÄT
WIEN
Vienna University of Technology

Diplomarbeit

Development of ICP-based methods for quantification of sulfur in electro- deposited copper samples

Ausgeführt am Institut für
Chemische Technologien und Analytik
der Technischen Universität Wien

Unter der Anleitung von
Privatdoz. Dipl.-Ing. Dr.techn. Andreas Limbeck

durch
Elke Ludwig, BSc.
Mat. Nr. 0802941
Taborstr. 93/79
1200 Wien

"En barndom utan böcker, det vore ingen barndom. Det vore att vara utestängd från det förtrollade landet, där man kan hämta den sällsammaste av all glädje."

"Eine Kindheit ohne Bücher wäre keine Kindheit. Es wäre, als ob man aus dem verzauberten Land ausgesperrt wäre, aus dem man sich die seltsamste aller Freuden holen könnte."

Astrid Lindgren

Abstract

Over the past 20 years, copper has become more and more important in the semiconductor industry. Its outstanding thermal conductivity, allowing miniaturization of chips, has led to a wide use in the microchip manufacturing process. During this process, by using different materials and components, variable layer structures can be manufactured. On silicon wafers, a copper layer is deposited on top to allow a better high temperature consistency, making use of its great thermal conductivity and low thermal expansion. Those wafers are used for microchips in power devices as used in e.g. cars or trains.

Deposition of copper layers on wafers can be derived through a sputtering process. Since this is no longer cost effective for layers thicker than 5 μm , a newer process for manufacturing of copper layer is via electroplating. For copper layers derived with this process, the addition of different additives to the liquid copper solution is needed to guarantee a homogeneous deposition. These additives contain sulfur. If sulfur is build-in into the copper layer during the electroplating process, it is a contamination, leading to different mechanical properties of the copper layer. Therefore analytical determination of the distribution and the total sulfur amount, in wafers manufactured through electroplating, are important.

Goal of this work was to determinate the sulfur content of several copper wafers. Analysis of sulfur using ICP (Inductively Coupled Plasma)–based methods is not very common. Different problems occur when analyzing sulfur using ICP-MS (Mass Spectrometry) or ICP-OES (Optical Emission Spectrometry).

One disadvantage of using ICP-MS is the occurrence of spectral interferences. For the analysis of sulfur on masses ^{32}S and ^{34}S spectral interferences occur, e.g. $^{16}\text{O}^{16}\text{O}$. Another problem is low ionization potential of sulfur.

Measuring with ICP-OES, spectral interferences seldom occur. However, sensitivity is much lower compared to ICP-MS, resulting in higher detection limits.

Existing measurement methods, especially for measuring sulfur in a metal matrix, are not widely spread or commonly used, resulting in non-satisfactory results. A thorough method development is required.

In this work the development and comparison of different ICP-techniques should be elaborated. Methods were developed and optimized using a stock solution for liquid measurements and self-manufactured pellets for solid-sample measurements. The copper wafers were analyzed as solid sample and after wet chemical dissolution measured on both ICP-MS and ICP-OES. To overcome interferences deriving from solvents, liquid ICP-MS measurements were conducted using a reactive cell, the reactive gas was O₂ and ¹⁶O ³²S was formed and detected on m/z = 48.

Results show that analysis of sulfur for liquid analysis is not possible without reaction cell technology for the ICP-MS. When using the reaction cell, limits of detection (LOD) for liquid sample analysis are almost the same using ICP-MS and ICP-OES. LOD around low ng/g were obtained. With this approach, sulfur contents for the copper wafers could only be determined using ICP-OES, since the WTi-layer of the wafers was also digested during sample preparation, leading to the detection of titanium on m/z = 48. Using ICP-OES, it was shown, that the different used additives lead to different sulfur contents, some of them under LOD. It was also shown, that the tempering process has influence on the sulfur content. Within the investigated wafer area, a homogeneous distribution was derived. For solid sample measurements much lower LOD was gained coupling the LA with ICP-MS than ICP-OES, deriving from the lower sensitivity of ICP-OES. Compared to liquid analysis, LA analysis is less sensitive. The big advantage of LA is that sample preparation is less work-intensive and no liquids are added. It also has better spatial resolution, allowing analysis of smaller sample-areas. The gained sulfur concentrations from liquid measurements were almost the same with LA-ICP-MS for the non-tempered wafer.

Kurzfassung

In den letzten 20 Jahren hat sich Kupfer in der Halbleiterindustrie zu einem immer wichtigeren Bestandteil entwickelt. Seine hervorragende Wärmeleitfähigkeit, erlaubt die Miniaturisierung von Chips. Dies hat zu einem breiten Einsatz in Mikrochip-Fertigungsprozessen geführt. Während dieser Prozesse, durch die Verwendung unterschiedlicher Materialien und Komponenten, können variable Schichtstrukturen hergestellt werden. Auf Silizium-Wafer wird auf der Oberfläche eine Kupferschicht abgeschieden um eine bessere Hochtemperaturbeständigkeit zu erzielen. Ermöglicht wird dies aufgrund der Nutzung der großen Wärmeleitfähigkeit und geringe Wärmeausdehnung von Kupfer. Diese Wafer werden für Mikrochips in Power-Geräten verwendet, wie z.B. in Autos oder Züge.

Kupferschichten auf Wafern können durch Sputter-Verfahren hergestellt werden. Da dies nicht mehr kosteneffektiv für Schichten dicker als 5 µm ist, gibt es ein neueres Verfahren zur Herstellung von Kupferschichten, des Galvanisieren. Um eine homogene Abscheidung von durch diesen Prozess erzeugten Kupferschichten zu gewährleisten, ist die Zugabe von verschiedenen Additiven zu der flüssigen Kupferlösung erforderlich. Diese Additive enthalten Schwefel. Wenn während der Herstellung Schwefel in der Kupferschicht eingebaut wird, kommt es zu Verunreinigungen. Diese führen zu veränderten mechanischen Eigenschaften der Kupferschicht. Daher ist die analytische Bestimmung der Verteilung und der Gesamtschwefelmenge im Wafer, welche durch Galvanisieren hergestellt werden, sind wichtig.

Ziel dieser Arbeit war es, den Schwefelgehalt von mehreren Kupferwafern zu bestimmen. Analyse von Schwefel mittels ICP (Inductively Coupled Plasma)-basierenden Methoden ist nicht sehr verbreitet. Verschiedene Probleme können bei der Analyse von Schwefel mittels ICP-MS (Mass Spectrometry) oder ICP-OES (Optical Emission Spectrometry) auftreten.

Ein Nachteil der Verwendung von ICP-MS ist das Auftreten von spektralen Interferenzen. Bei der Analyse von Schwefel auf den Massen ^{32}S und ^{34}S treten spektrale Interferenzen auf, z.B. $^{16}\text{O}^{16}\text{O}$. Ein weiteres Problem ist das geringe Ionisationspotential von Schwefel.

Bei der Messung von Schwefel mit der ICP-OES, gibt es kaum spektrale Interferenzen. Jedoch ist die Empfindlichkeit dieser Messmethode geringer als jene verglichen mit ICP-MS. Dies resultiert in höheren Nachweisgrenzen.

Bestehende Messmethoden, insbesondere zur Messung von Schwefel in einer Metallmatrix sind nicht weit verbreitet oder angewendet. Dies führt zu nicht zufriedenstellenden Ergebnissen führt. Eine gründliche Methodenentwicklung erforderlich ist.

In dieser Arbeit sollten die Entwicklung und der Vergleich von verschiedenen ICP-techniken erarbeitet werden. Methodenentwicklung und –optimierung erfolgten mit einer Standardlösung für Flüssigmessungen und selbst hergestellten Presslingen für Festkörpermessungen. Die Kupferwafer wurden als feste Probe und, nach nass-chemischer Auflösung, mit ICP-MS und ICP-OES analysiert. Interferenzen der flüssigen ICP-MS Messung, welche aus Lösungsmitteln und Wasser stammen, wurden umgangen indem die Messungen mit einer Reaktionszelle durchgeführt wurden. Als reaktives Gas wurde O₂ verwendet und das gebildete ¹⁶O ³²S wurde auf m/z = 48 detektiert.

Die Ergebnisse zeigen, dass die Flüssigmessung von Schwefel ohne Reaktionszelle mit ICP-MS nicht möglich ist. Bei Verwendung der Reaktionszelle sind Nachweisgrenzen für die Flüssiganalyse von ICP-MS und ICP-OES nahezu gleich. Nachweisgrenzen befinden sich im niedrigen ng/g-Bereich (ppb). Im Zuge dieser Arbeit konnten die Schwefelgehalte der Flüssigmessung für die Kupferwafer jedoch nur mit ICP-OES bestimmt werden, da die WTi-Schicht der Wafer während der Probenvorbereitung mit aufgelöst wurde. Dies führte zur Detektion von Titan auf m/z = 48. Mit ICP-OES-Analyse konnte gezeigt werden, dass die verschiedenen beim Herstellungsprozess verwendeten Additive zu unterschiedlichen Schwefelgehalten der Wafer führen, einige von ihnen sogar unter der Nachweisgrenze liegen. Auch, dass der Temperprozess Einfluss auf den Schwefelgehalt hat konnte ermittelt werden. Innerhalb des untersuchten Wafer-bereichs wurde eine homogene Verteilung für den Schwefel erhalten. Für feste Probenmessungen wurden niedrigere Nachweisgrenzen für Schwefel bei der Kopplung des Lasers mit ICP-MS erhalten als bei der Kopplung des Lasers mit ICP-OES. Dies lässt sich aus der geringeren Empfindlichkeit der ICP-OES ableiten. Im Vergleich zu Flüssigkeitsmessungen ist LA (Laser Ablation) jedoch weniger empfindlich. Der große Vorteil der Laser Ablation ist, dass die Probenvorbereitung weniger arbeitsintensiv ist und keine Flüssigkeiten eingebracht werden. Des Weiteren erhält man bessere Auflösung, so dass die Analyse kleinerer Probenbereiche möglich ist. Für die ungehärteten Wafer waren die erhaltenen Schwefelkonzentrationen von Flüssigmessungen und jene erhalten mit ICP-MS waren sehr ähnlich.

Acknowledgement

The past six years at Vienna University of Technology have enriched my life with the access to a high quality education and the opportunity to meet interesting people on the way.

First I want to thank my supervisor Andreas Limbeck for the offer to work in his group, his valuable support and dedicated input, which he contributed with to my master's thesis. The working group I want to thank for making this experience such a wonderful and fun one.

I want to thank KAI for making this work possible.

Max Bonta I want to thank for the patience. He helped me to overcome many practical obstacles in the project and we had lots of fun together. Viktor Bauer for being my partner-in-crime, spending long days together, studying, laughing, supporting each other, for being an amazing friend. Moreover I want to thank my colleagues from University: Christoph, Dodo, Elise, Anja, Silvia, Melanie, Michi and Hannes, and all the others who all contributed to this journey.

Furthermore I want to thank my friends from outside the University: Claire Brenner for being by my side since so many years and for all of our fruitful, fun, loving Thursday evenings, as well as Irini, Nisse, Jessica, Tess, Livi, Bea, Michaela, Isi, Esther and Lena.

My partner Patrick Pikes for always believing in me, even in times when I lost faith in myself he did not.

Last but not least I want to thank my family for always supporting, helping and loving me, no matter what.

So thank you all from the bottom of my heart, for making this wonderful journey possible and for giving me some incredible memories.

Table of Content

| | |
|---|-----|
| Abstract | III |
| Kurzfassung | V |
| Acknowledgement | VII |
| Abbreviations..... | X |
| Introduction..... | 11 |
| 1. Theory..... | 14 |
| 1.1. Copper Wafer | 14 |
| 1.2. Laser Ablation (LA)..... | 15 |
| 1.3. Inductively Coupled Plasma (ICP) | 17 |
| 1.4. Inductively Coupled Plasma Mass Spectrometry (ICP-MS)..... | 19 |
| 1.4.1. Sample Introduction | 19 |
| 1.4.2. Inductively Coupled Plasma (ICP)..... | 19 |
| 1.4.3. Interface | 20 |
| 1.4.4. Ion Focusing System | 21 |
| 1.4.5. Mass Analyzer..... | 22 |
| 1.4.6. Detector | 24 |
| 1.4.7. Measurement of Sulfur | 24 |
| 1.4.8. Collision Cell Technology (CCT) | 26 |
| 1.5. Inductively Coupled Plasma Optical Emission Spectrometry (ICP-OES) | 28 |
| 1.6. Time of Flight-Secondary Ion Mass Spectrometry (TOF-SIMS) | 30 |
| 2. Experimental..... | 31 |
| 2.1. Samples and preparation | 31 |
| 2.1. Instrumentation | 32 |
| 2.2. Preparation of Pellets | 37 |

| | | |
|--------|--|----|
| 2.3. | Digestion of Copper Wafers | 39 |
| 2.4. | Preparation of Standards | 39 |
| 2.4.1. | Standards for Calibration | 39 |
| 2.4.2. | Matrix Matched Calibration | 40 |
| 2.5. | TOF-SIMS | 40 |
| 3. | Results and Discussion..... | 42 |
| 3.1. | Method Development for Liquid Measurements..... | 42 |
| 3.1.1. | ICP-MS, Comparison Standard-mode vs CCT-mode | 42 |
| 3.1.2. | ICP-OES..... | 43 |
| 3.2. | Method Development for Solid Measurements..... | 44 |
| 3.2.1. | Pellets, Preparation of Sulfur Containing Copper Standards for LA Calibration Measurements..... | 44 |
| 3.2.2. | LA-ICP-OES | 47 |
| 3.2.3. | LA-ICP-MS | 48 |
| 3.3. | Results Wafer | 51 |
| 3.3.1. | Liquid | 52 |
| 3.3.2. | Solid, LA-ICP-MS | 58 |
| 3.3.3. | SIMS..... | 60 |
| 4. | Conclusion and Outlook..... | 62 |
| | References..... | 64 |
| | List of figures | 66 |
| | List of tables..... | 68 |
| | Appendix | 69 |

Abbreviations

| | |
|---------|--|
| CCT | Collision Cell Technology |
| GDMS | Glow Discharge Mass Spectrometry |
| ICP-MS | Inductively Coupled Plasma Mass Spectrometry |
| ICP-OES | Inductively Coupled Plasma Optical Emission Spectrometry |
| LA | Laser Ablation |
| LOD | Limit of Detection |
| LOQ | Limit of Quantification |
| MMC | Matrix Matched Calibration |
| m/z | mass-to-charge ratio |
| Q-MS | Quadrupole Mass Spectrometry |
| RSD | Relative Standard Deviation |
| SEM | Scanning Electron Microscopy |
| SIMS | Secondary Ion Mass Spectrometry |
| TOF | Time of Flight |

Introduction

In the semiconductor industry, copper is a widely used material. Its high thermal conductivity, low thermal expansion and its hardness are some of the advantages supplied by this material. For production of copper layer wafers, organic additives are added. These additives increase epitaxial growth characteristics and contain sulfur.¹ They are incorporated in the copper layer electroplates, where sulfur migrates to the grain boundaries of copper grains, leading to worse mechanical properties. It also inhibits the possibility for grain growth.

The question arises if different additives result in different sulfur concentration, leading to altered properties of the copper layers. To answer this question copper plates, manufactured with different additives were analyzed.

Sulfur is widely distributed in the environment. It occurs in earth spheres, many ores, such as CuFeS_2 (chalcopyrite), ZnS (sphalerite), PbS (galenite) etc., in enzymes, microorganisms, fuels and many more. Analytical detection of sulfur in major- and trace element concentration is therefore very important in several application fields, e.g. analysis of sulfur in biological materials, in metallurgy material, in fuels, etc. Common methods used for quantification are combustion bombs or tubes where SO_2 is detected, wavelength dispersive- or energy dispersive-X-ray fluorescence spectrometry. All these methods have their disadvantages, such as matrix related interferences, accuracy, high detection limits and non-simultaneous-multielement-analysis.^{2,3} Thus, these techniques are not suitable for the analysis of sulfur in copper samples.

Inductively coupled plasma optical emission spectrometry (ICP-OES) is mainly used for analysis of liquid samples. It has the big advantage of simultaneous multielement analysis and is a robust and reliable analytical technique that can be applied for the determination of many metals as well as non-metals.⁴ This technique is one of the techniques currently used for sulfur analysis.

Inductively coupled plasma mass spectrometry (ICP-MS) is a very sensitive and accurate detection technique. It is capable of measuring most of the elements and providing high sample throughput.

¹ (Robl, Melzl, Weidgans, Hofmann, & Stecher, 2008)

² (Mason, Kaspers, & Bergen, 1999)

³ (Pereira, et al., 2009)

⁴ (Santelli, Oliveira, de Carvalho, Bezerra, & Freire, 2008)

Isotopic information can be gained by analyzing samples with ICP-MS. Quantification as well as qualification can be gained using this technique. Detection of sulfur however is not that straightforward. There are major factors that hinder the artlessness of sulfur analysis with ICP-MS. One of them is the formation of spectral interferences (polyatomic oxygen species) on m/z (mass-to-charge ratio) ^{32}S and ^{34}S .⁵

Different approaches can be applied to avoid spectral interferences. The more common one is the usage of a reaction cell. This method is used when analyzing liquid samples, since the oxygen for the formation of $^{16}\text{O}^{16}\text{O}$ is provided from the water and acids in the aqueous solutions. When using a reactive cell, a reactive gas, such as O_2 or N_2 , is pumped into the cell, mostly a quadrupole or multipole, where the gas reacts with the sample ions that were derived in the plasma. New molecules form and can be detected on a different mass than the analyte ion.

Both ICP-MS and ICP-OES require sample preparation for almost every sample before liquid analysis. This means dissolving and diluting solid samples, which are one or more time consuming steps that often can lead to contaminations and dilution errors.

In solid state analytics, there are different state of the art procedures for sulfur analysis. For example SEM (Secondary Electron Microscope). SEM can be used for quantification, qualification and distribution analysis, but has the disadvantage of low sensitivity, making it a non-suitable technique for sulfur analysis in copper wafers. Another approach is the usage of GDMS (Glow Discharge Mass Spectrometry), delivering low LOD's and is suited for qualification as well as quantification, but not being able to provide lateral information of the analyte. Also SIMS (Secondary Ion Mass Spectrometry) should be mentioned, being a good technique for the provision of distribution and depth profiles, but lacking the possibility of quantification without matching reference material.

When using ICP-MS or ICP-OES, another approach is the application of LA (Laser Ablation). LA is an instrument that makes it possible to analyze solid samples without sample treatment. A laser beam of a 213 nm Nd:YAG laser is directed onto the solid sample. Through the local energy input

⁵ (Prohaska, Latkoczy, & Stingeder, 1999)

the sample is ablated and transported into the plasma. A drawback of using LA is the availability of reference materials. Due to the occurrence of matrix effects, the material for calibration should consist of the same or similar matrix as the sample to be analyzed. Since that is mostly not accessible, a manufacturing process has to be established.

Both of the above named ICP-MS methods were applied in this work. They are not very well tested for the determination of sulfur. Gaining accurate information and reliable quantitative information is in most cases a complex challenge.

In this work a comparison between liquid measurements with ICP-MS and ICP-OES of copper electroplates, with different additives, and solid measurements with ICP-MS should be provided. Comparison should show if the step of sample preparation brings advantages or disadvantages and if both inductively coupled plasma techniques purvey the same result.

LA-ICP-MS analysis is used for quantification of sulfur, as well as to determinate if a homogeneous distribution of sulfur is obtained during the electroplating process of the copper wafers. For comparison liquid ICP-MS and ICP-OES measurements are conducted. When analyzing liquid samples a higher sensitivity can be derived, making it a suitable comparison method.

1. Theory

1.1. Copper Wafer

The manufacturing of copper wafers was previously done via sputtering. This production method however is no longer cost effective for layers thicker than 5 μm . A good alternative to sputtering is electroplating. Yet the difference in the properties of sputtered and electrochemical deposited copper layers is a key question in the semiconductor industry.

During the manufacturing process of copper electroplates, a direct-current voltage is applied to the electrolyte bath resulting in dissolution of copper at the anode (positive pole, +), Cu^{2+} is generated. These copper ions migrate through the electrolyte solution toward the negative pole, the cathode(-). There the Cu^{2+} ions are electro-deposited as Cu^0 , forming the metal surface of the copper wafer. Electroplated copper is derived from a solution which is composed of several components. The solution contains both inorganic compounds ($\text{CuSO}_4 \cdot 5 \text{H}_2\text{O}$, H_2SO_4 , HCl) as well as organic additives. Additives are sectioned into three different parts:

- Suppressor: a large, long-chained organic molecule, often polyethylene glycol ($[\text{C}_2\text{H}_4\text{O}]_n$), that forms a complex with Cu^+ and Cl^- ions. The originated complex adsorbs to the copper surface and inhibits deposition at edges and therefore thickness uniformity is improved.
- Accelerator: the accelerator is a small molecule (Bis-(sodium sulfopropyl)-disulfide ($\text{C}_6\text{H}_{12}\text{Na}_2\text{O}_6\text{S}_4$)) that locally suspends the effect of the suppressor and acts as a grain refiner. Therefore a homogeneous layer growth is enabled.
- Leveler: the leveler is a form of a strong suppressor. It adsorbs at areas with high current densities. There it prohibits exceeding layer growth. It usually consists of nitrogen compounds.

The addition of additives plays an important role in the electroplating process of copper. They help to obtain a consistent and even layer growth. Layers derived from electrolyte solutions without additives are much rougher and different layer thicknesses can occur. Another advantage of additive usage is the lower sensibility towards alterations in the current-density, which can e.g. occur on edges.^{6,7} In this work copper wafers, each manufactured with one of four different additives are to be analyzed.

⁶ (Robl, Melzl, Weidgans, Hofmann, & Stecher, 2008)

1.2. Laser Ablation (LA)

A method for solid sample analysis is laser ablation. For LA the sample is placed in a so called ablation chamber. The ablation chamber is airtight and purged with a carrier gas, such as helium or argon. The laser beam is focused and then applied on the sample. Through thermal heating, particles are dissolved from the sample surface generating a fine vapor aerosol. The vapor and particulate matter is carried through an ablation cup into the plasma with the carrier gas. When reaching the plasma the ionization process takes place. Set-up of a laser ablation system is illustrated in Figure 1. The spot diameter of the laser beam can be varied, leading to a spatial resolution between 5 to 250 μm , allowing almost nondestructive analysis of valuable samples when using smaller diameters.

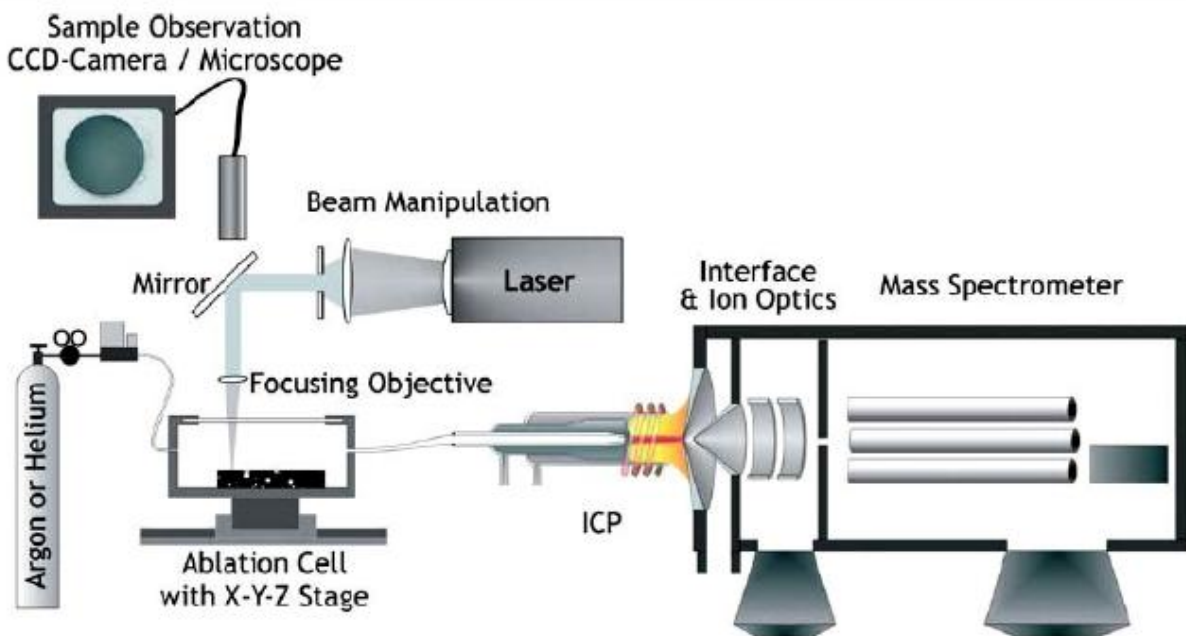


Figure 1: Set-up of a LA system, coupled with an ICP-MS⁸

Some of the major influences on the vaporization and ionization are laser-wavelength, carrier gas, carrier gas flow, pulse duration, pulse energy and particle size. Wavelengths of most common lasers are located in the UV-range (266, 213 and 193 nm). Shorter wavelengths result in a reduced thermal alteration of the sample material during the ns-laser pulse. More widespread use of fs-

⁷ (Larisegger, 2014)

⁸ (Günther & Hattendorf, 2005)

lasers is currently limited by the high prices of these instruments. With metallic samples however it seems, that the pulse duration has more of an impact on the ablation characteristics than the wavelength. It was also shown, that using helium as carrier gas, results in a signal enhancement. Signal intensity is directly proportional to the amount of ablated material transported into the ICP. Leading to better detection limits for bigger laser diameters.

Fields of applications are broad. Laser ablation is used for geological, biological, forensic samples and many more.^{9,10}

Analyzing the sample in its natural stage brings several benefits, such as minimization of contamination, elimination of dilution errors and loss of volatile elements. LA is a method that analyzes samples without sample preparation of solid samples. When analyzing a sample, using small laser diameters the distribution of the analyte can be obtained. Using large diameters results in bulk information. It is important that not too little of a sample is ablated and analyzed, because if the sample is inhomogeneous the result is not representative for the whole sample. Solutions are homogenous and it is easier to take up a larger amount of sample leading to a valid representation of the bulk sample.

A limitation of laser ablation is that the calibration typically requires matrix-matched standards, since the ablation rate varies with sample matrix. Using different matrices results not only in different ablation, but also in different absorption, leading to different sample input into the plasma. This is called matrix effects.

Quantification for solid samples is usually not that easy. Since matrix dependent ablation effects are known to occur when analyzing solid samples via LA, reference material with similar matrices to the samples need to be measured to generate a calibration. However, reference materials are not commercially available for all the different matrices. Often reference materials have to be produced in-house.

⁹ (Günther & Hattendorf, 2005)

¹⁰ (Mokgalaka & Gardea-Torresdey, 2006)

1.3. Inductively Coupled Plasma (ICP)

Inductively coupled plasma (ICP) has become of common use in analytical atomic spectroscopy. It is routinely applied for the quantification and qualitative analysis of very diverse materials.

The plasma is formed in a stream of argon-gas. The gas flows through the plasma torch, consisting of three concentric quartz tubes. The torch is designed to adhere a homogenous gas flow, which results in stable plasma conditions. The goal is to maintain constant temperature in the plasma and therefore gain a reproducible method.¹¹ The plasma torch is enwrapped by an induction coil which is connected to a radiofrequency (RF) generator and cooled with argon gas. For the cooling gas, a second stream of gas usually is needed to cool down the inside of the quartz tube. This is provided by a stream of argon that provides a vortex flow. The flow also centers and stabilizes the plasma¹². For the composition of the plasma torch, see Figure 2.

A stable plasma is sustained as long as the argon gas flow is continuous and the magnetic field strength is adequate. In the plasma the molecules are first vaporized, then atomized, excited and last ionized. Depending on the device emitted radiation (ICP-OES) or ions (ICP-MS) are detected. Some of the main characteristics of the argon ICP are: plasma temperature between 6000 - 10000 K depending on the HF energy and applied gas flow, high electron number density ($1-3 \times 10^{15} \text{ cm}^{-3}$). Residence time of the sample aerosol in the plasma is about 2 - 3 ms and that the process of the vaporization to atomization happens in a nearly chemically inert environment. Due to these properties, the argon ICP is commonly used for simultaneous multielement analysis. Argon ICP makes it possible to detect a wide variety of elements down to trace- and ultratrace concentration levels, with the advantage of low-noise conditions.

The principle of ICP is, that a gaseous, liquid or solid sample is transformed into an aerosol and transported into the plasma. The analytes are introduced either as a wet aerosol produced from a liquid sample, or a dry aerosol from a solid sample. The aerosol is carried into the plasma via a carrier gas through the inner tube of the plasma torch and transported into the argon plasma. In the plasma the vaporization-atomization-excitation-ionization, depending on the plasma temperature, process takes place.

¹¹ (Nischkauer, 2011)

¹² (<http://em-1.stanford.edu/Schedule/ICP/abouticp.htm>)

The plasma temperature varies depending on the position in the plasma, see Figure 2.

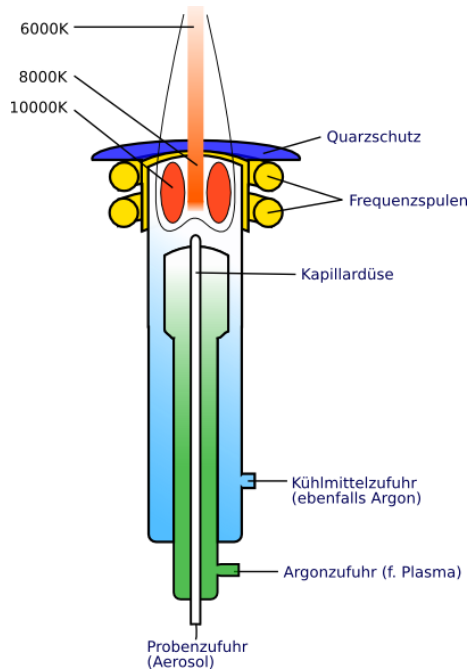


Figure 2: ICP Torch¹³

The high plasma temperature, that automatically leads to a high gas and high electron temperature, as well as the long dwell time of the sample in the plasma results in a nearly complete excitation-ionization of the sample aerosol. Also the chemical and physical interferences are reduced.

Usage of an argon ICP spectrometer offers different advantages, such as low detection limits, low relative standard deviation (0,2 – 3% RSD) and the possibility to detect almost all elements.

Both analysis methods that were used in this line of work, ICP-MS and ICP-OES, have in common that the sample is converted into an aerosol. The main difference between these two methods appears after the argon plasma. Whilst in the ICP-MS the ionized atoms are extracted into high vacuum, where they are focused and transmitted into a mass analyzer, the ICP-OES detects the

¹³ (<http://upload.wikimedia.org/wikipedia/commons/3/3d/ICP-Brennerduese.png>)

radiation emitted by the excited analytes. Both have a wide range of use e.g. environmental, geological and biological analysis.

The two different methods are further explained in chapters Inductively Coupled Plasma Mass Spectrometry (ICP-MS) and Inductively Coupled Plasma Optical Emission Spectrometry (ICP-OES).

1.4. Inductively Coupled Plasma Mass Spectrometry (ICP-MS)

Inductively coupled plasma mass spectrometry (ICP-MS) has become an important analysis method for inorganic trace- as well as ultra-trace analysis over the last years. Its low detection limits, down to ppt-scale (pg/L), the simultaneous multielement analysis, high sensitivity and the high dynamic range of the instrument are some of the factors that distributed to the frequent use of ICP-MS. Another great benefit is the possibility of isotope analysis.

1.4.1. Sample Introduction

Sample introduction into the plasma plays a key role in the production of ions and interfering species. In case of LA-ICP-MS the aerosol is formed via the thermal heating of the laser beam and transported into the plasma with a carrier gas.

Most samples exist as liquids, making this the most common way of sample introduction. With liquid sample introduction, the sample is converted into an aerosol via a nebulizer and then passes through a peltier-cooled spray chamber, where the big aerosol drops are separated from the small ones, and only those are transported into the plasma, since smaller drop diameters are easier to evaporate, leading to more effective ionization of the sample. In this work, a concentric pneumatic nebulizer and a cyclonic spray chamber were used. A benefit of liquid sample introduction is the simplicity of calibration for quantification.

Another technique for sample transport into the plasma is via gas phase. The analytes are transferred into a gas phase and then introduced into the ICP, for example through coupling with a gas chromatograph (GC) or supercritical fluid chromatography (SFC).

1.4.2. Inductively Coupled Plasma (ICP)

As described in Chapter 1.3 a plasma is generated. In the plasma the molecules dissociate and the atoms are ionized. The plasma contains a temperature gradient, see Figure 2. In the hotter regions ions are formed, whereas in cooler regions re-association or the formation of polyatomic ions can occur, e.g. between analyte ions and oxygen, nitrogen or argon atoms or ions. These

polyatomic ions often have similar masses as other single atomic ions and are therefore detected on the same mass. This effect can seldom be disabled and is called spectral interferences. To avoid falsified results, it is advisable to measure more than one isotope of the analyte, making it possible to look at the isotope ratio and seeing if the ratio fits and the measured ions are only analytes or if spectral interferences appear.

1.4.3. Interface

Inductively coupled plasmas are operated under atmospheric pressure, whilst the detection of the ions, in an ICP-MS, is carried out under high vacuum that needs to be higher than 10^{-5} mbar, usually it varies between 10^{-7} to 10^{-8} mbar. The high vacuum is necessary to reduce the number of gas molecules, resolving in lesser collisions with analyte ions leading to increased transmission. For coupling atmospheric pressure and high vacuum an intermediate region is needed and provided by the MS Interface.

The Interface consists of two stages, called the sampler- and skimmer-cone. The built up of an ICP-MS interface is illustrated in Figure 3. Both cones consist of metal, often nickel or, for special applications, platinum cones can be used. The first cone, sampler cone, is the barrier into an intermediate vacuum zone, with a pressure around 1 mbar. Behind the sampler cone the second cone, the skimmer cone, is placed. It transitions the intermediate vacuum into high vacuum. The diameter of the hole of the skimmer cone is approximately 1 mm and should be as large as possible to maximize analyte signal and minimize orifice clogging while keeping the extraction pumps small.

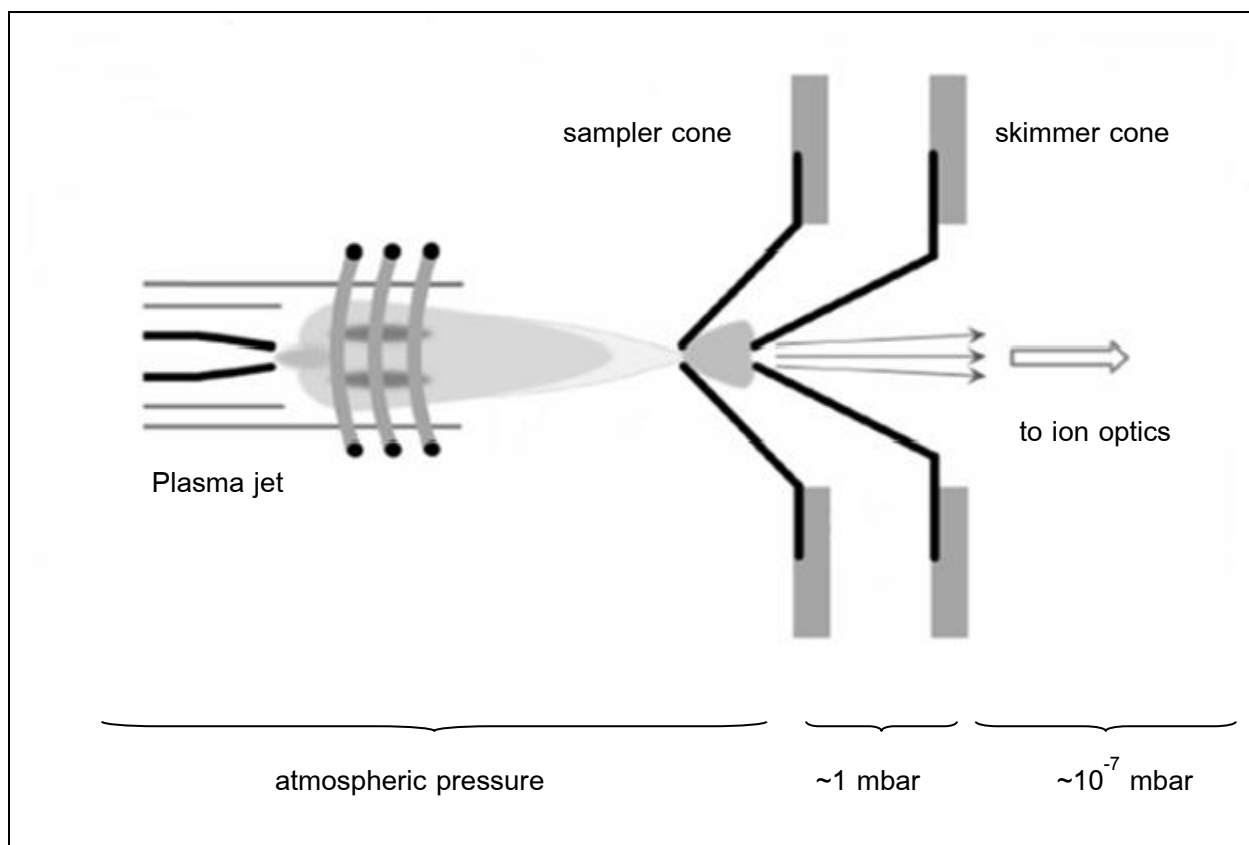


Figure 3: Vacuum interface, ICP-MS¹⁴

1.4.4. Ion Focusing System

The ion focusing system is an essential part in the ICP-MS. It is located after the skimmer cone and has the important task of focusing the ion beam before it enters the mass analyzer. When the ions are extracted from the plasma into high vacuum, the ions enter into the vacuum unfocused. To refocus the ions into a beam once again, the ion optic system is installed.

The ion optics consist of one or more ion lenses, which navigate the analytes electrostatically from the interface into the MS. The goal of the ion focusing system is to transport the maximum number of analyte ions into the MS and at the same time reject as many of the matrix- and non-analyte-based (e.g. photons) components as possible. The second major function of the ion optics consists in stopping particles, neutral species and photons from entering into the mass spectrometer device, as these components lead to high background noise if they reach the detector. For that task a metallic disc, a so called “photon stop” is placed at the center of the lens system. This photon stop

¹⁴ (Bonta, 2013)

prohibits a direct line of sight between the detector and the plasma and prevents plasma produced photons from reaching the detector. Low background counts, better detection limits and stable signals are enabled because of the ion focusing system.¹⁵ Another instrument set-up to stop unwanted species from reaching to detector is application of a 90° deflection lens. Analyte ions are deflected towards the detector, arranged 90° from the primary ion beam, photons and other unwanted species are not deflected, therefore never reaching the detector.

1.4.5. Mass Analyzer

Separating the ions according to their mass-to-charge ratio is achieved with a mass separation device. The main goal is to divide the analytes from the ions that are of no interest, such as matrix, solvent etc. Depending on the mass analyzer, the selection process is accommodated in different ways. Currently there are three different types of mass analyzers available: quadrupole MS, sector field MS and time-of-flight (TOF) MS. Whereof the first one is by far the most common mass separation device. TOF-MS were only commercially available for a short period. All of the mass separation devices are placed between the ion focusing system and the detector.

For the experiment presented in this master's thesis a quadrupole mass analyzer was used, therefore only quadrupole will be described more detailed.

Q-MS are widely used because of their relative simplicity, good performance, high-throughput and low cost. As illustrated in Figure 4, a quadrupole is build-up of four cylindrical metal rods, made of stainless steel or molybdenum, sometimes with a ceramic coating for corrosion resistance. Their dimensions are about 1 cm in diameter and 15 to 20 cm in length.

¹⁵ (Thomas, A Beginner's Guide to ICP-MS, Part V: The Ion Focusing System, 2001)

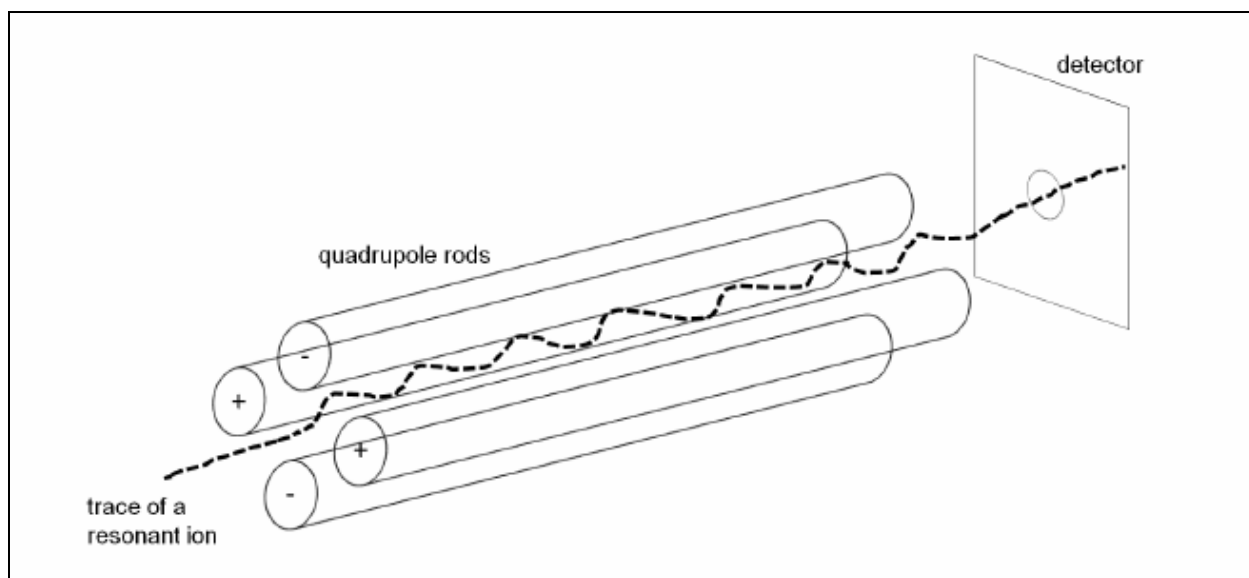


Figure 4: Quadrupole mass separation device¹⁶

When ions enter the quadrupole a direct current field is applied on one pair and a radio frequency field on the other pair of rods. This results that only ions of one selected m/z are allowed to pass through the quadrupole, the others are rejected. As soon as a particular voltage is applied to the rods, the positive or negative bias that is generated will electrostatically guide the analyte ion down in the middle of the four rods to the end. When the ion emerges it is converted into an electrical pulse and registered by the detector. The ions of no interest, meaning having different mass-to-charge ratios, will pass through the spaces between the rods and be ejected from the quadrupole. This sequence is repeated for every m/z wished to be analyzed.¹⁷

Yet quadrupoles have their limitations, being sequential instruments, having relatively low resolution. This low resolution derives from peaks that cannot be separated. For achieving higher mass resolution, application of a sector field is necessary, serving as high resolution mass analyzers. Time-of-flight mass separation devices allow simultaneous detection of the whole mass spectrum.

¹⁶ (Bonta, 2013)

¹⁷ (Thomas, A Beginner's guide to ICP-MS, Part VI- The Mass Analyser, 2001)

1.4.6. Detector

After leaving the mass analyzer unit, the ions arrive at the detector. There the arriving ions are converted into electrical pulses which are counted. The magnitude of electrical pulses is proportional to the number of ions reaching the detector.

In most cases the detector is an electron multiplier. In an electron multiplier, the ion enters the detector and impacts on either a semiconductor material (channel electron multiplier) or on discrete dynodes (discrete dynode electron multiplier), generating electrons. These electrons start a chain reaction, generating more and more electrons, hence causing a multiplication of the signal.¹⁸

1.4.7. Measurement of Sulfur

Ionization of nonmetals in the argon plasma is relatively little. This is a disadvantage, making the ICP more insensitive for analyzing nonmetallic compounds than metallic compounds. Still, the limit of detections that can be achieved for some nonmetals, are much lower than with many other analyzing methods.

One alternative to achieve higher ionization of nonmetals is the usage of helium plasma instead of argon plasma.

Quantification of sulfur with ICP-MS proves to be difficult. Three major reasons are responsible for that:

- The 1st ionization potential of sulfur ($S \rightarrow S^+ + e^-$, 999.6 kJ/mol) is above that of all metals and approaches the ionization potential of the plasma gas, argon (1520.6 kJ/mol). This high ionization energy leads to poor ionization efficiency of sulfur in argon plasma.¹⁹
- Many polyatomic interferences on m/z 32 and 34 (^{32}S and ^{34}S) appear. The most common ones are listed in Table 1. Oxygen sources are most often derived from the sample matrix (solvent, acid, water) or ambient air.
- Blank levels for sulfur ^{32}S and ^{34}S are high. Not all reasons for that are known, it is assumed that contaminations, for example sulfur in the oil of the ICP-MS cooler are responsible for high blank levels.²⁰

¹⁸ (Thomas, A Beginner's Guide to ICP-MS, Part X- Detectors, 2002)

¹⁹ (Mason, Kaspers, & Bergen, 1999)

An additional reason for high detection limits is the relative lightness of sulfur, not allowing it to be as efficiently transmitted into the MS by typical instrumental ion optics as heavier masses.

Table 1: Spectral interferences at m/z 32 and 34²¹

| Isotope | Interferences | Abundance [%] |
|-----------------|---|---------------|
| ³² S | ¹⁶ O ¹⁶ O | 95.02 |
| | ¹⁴ N ¹⁸ O | |
| | ¹⁴ N ¹⁶ O ¹ H ¹ H | |
| ³⁴ S | ³² S ¹ H ¹ H | 4.2 |
| | ¹⁶ O ¹⁸ O | |
| | ¹⁶ O ¹⁶ O ¹ H ¹ H | |

A relatively new approach to avoid these polyatomic interferences is the application of a collision/reaction cell. When using a collision/reaction cell with oxygen as reactive gas, ³²S is quantified on m/z 48 as ³²S¹⁶O. This makes it possible to quantify sulfur practically interference-free. Detection limits down to 0.2 µg/L can be achieved with this method.²² However, this approach is only possible if the sample does not contain titanium, m/z = 48, because it will interfere with the ³²S¹⁶O signal. This procedure should be evaluated in this master's thesis.

When using ICP-MS instruments, other approaches to solve the problem of sulfur analysis are e.g. reduction or elimination of the solvent load of the nebulized solution by alternative sample introduction, such as electro-thermal vaporization. Sulfur isotope measurement via high resolution ICP-MS has achieved low detection limits down to 100 ng/L.²³ Application of double- focusing sector field ICP-MS is another way to overcome spectral interferences. Because of the higher resolution the ¹⁶O¹⁶O peak can be separated from the ³²S peak. However this type of instrument comes at significantly higher costs than a quadrupole ICP-MS. This approach brings another disadvantage, reducing the ion transmission efficiency by 10-fold, leading to much lower signal intensity. Recently developed 'triple quadrupole' MS instruments can also be used for detection of sulfur without spectral interferences, when operated in the MS/MS-mode. A triple quadrupole (ICP-

²⁰ (Guillong, Latkoczy, Hun Seo, Günther, & Heinrich, 2008)

²¹ (Prohaska, Latkoczy, & Stingeder, 1999)

²² (Balcaen, Woods, Resano, & Vanhaecke, 2012)

²³ (Mason, Kaspers, & Bergen, 1999)

QQQ-MS) is build up of two quadrupole analyzers and in between those two an octopole-based collision/reaction cell is placed. Operated in the MS/MS-mode, the first quadrupole prevents all off-mass ions from entering the collision/reaction cell, resulting in more controlled and efficient interference removal.²⁴ One last approach in bypass spectral interferences should be named. Using Xenon (Xe) as reactive gas, interfering O^{2+} ions can be reduced considerably, but the overall sensitivity decreases.^{25 26} ,

1.4.8. Collision Cell Technology (CCT)

Some elements are observed to have poor detection limits when analyzed with an ICP-MS. Taking a closer look, it can be observed, that these elements suffer from major polyatomic interferences. Some of these are: $^{40}Ar^{16}O$ on ^{56}Fe , ^{38}ArH on ^{39}K and, playing an important role in this thesis, $^{16}O^{16}O$ on ^{32}S .

Due to the formation of polyatomic spectral interferences, see chapter 1.4.2, the detection potential for some critical elements is severely limited. One way to bypass these interferences is by applying a so called reaction- or collision cell (CC).

As illustrated in Figure 5, the collision cell is placed after the ion optics and before the analyzer quadrupole. After leaving the ion focusing device the generated ions enter directly into the CC. The collision cell consists of a multipole, usually a quadrupole, which is operated by using radio frequency.

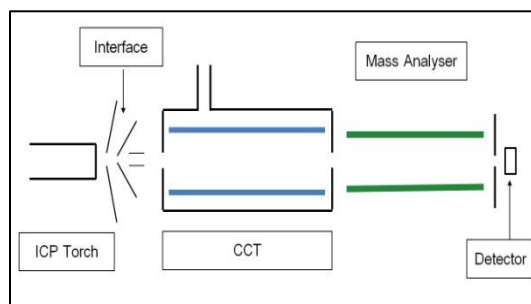


Figure 5: Collision cell, empty

²⁴ (Balcaen, Woods, Resano, & Vanhaecke, 2012)

²⁵ (Mason, Kaspers, & Bergen, 1999)

²⁶ (Guillong, Latkoczy, Hun Seo, Günther, & Heinrich, 2008)

When the ions enter the collision cell, a collision/reaction gas is added. Gases used are H, He, O₂, NH₃ etc. Depending on the character of the gas, it will either act as a reactive gas, forming a new molecule or it will act as a collision gas, eliminating polyatomic ions.

Due to radio frequency appliance only, the masses are not separated in the collision cell. Instead the effect of focusing the ions occurs, leading to collision and reaction between the ions and the reaction/collision gas. Because formation of many interfering species occurs inside the reaction/collision cell, ways of elimination or rejection are needed. There are two approaches used to separate the unwanted ions from the analytes:

- discrimination by kinetic energy

- discrimination by mass.²⁷

One advantage of separating interferences is improved selectivity, but it comes at the cost of reduced sensitivity.

Figure 6 to Figure 8 show what happens inside the collision cell, when a reacting gas is used. Here the reacting species are sulfur and oxygen. Sulfur ions enter the CC, where O₂ is added as reaction gas. S and O form SO, leaving the collision cell, entering the quadrupole and from there the detector.

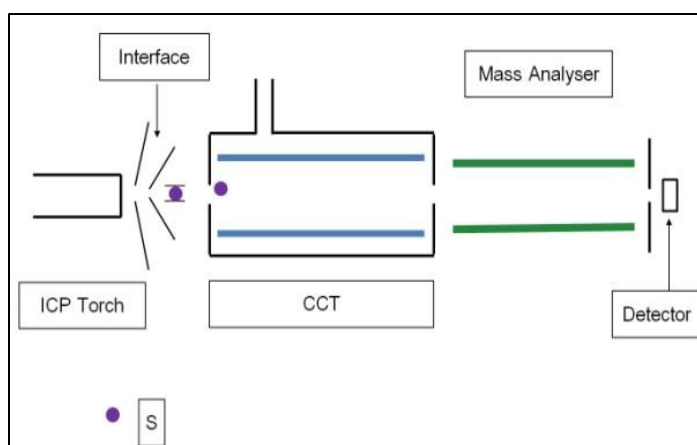


Figure 6: Collision cell, sulfur ions enter into the cell

²⁷ (Thomas, A Beginner's Guide to ICP-MS, Part IX - Mass Analyzers: Collision/Reaction Cell Technology, 2002)

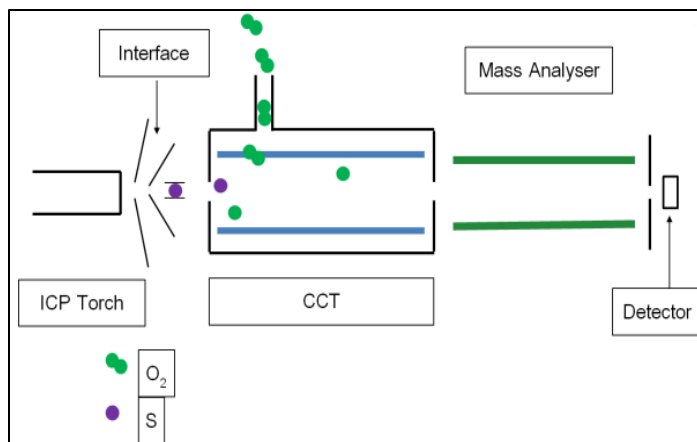


Figure 7: Collision cell, sulfur ions and O₂ as reactive gas

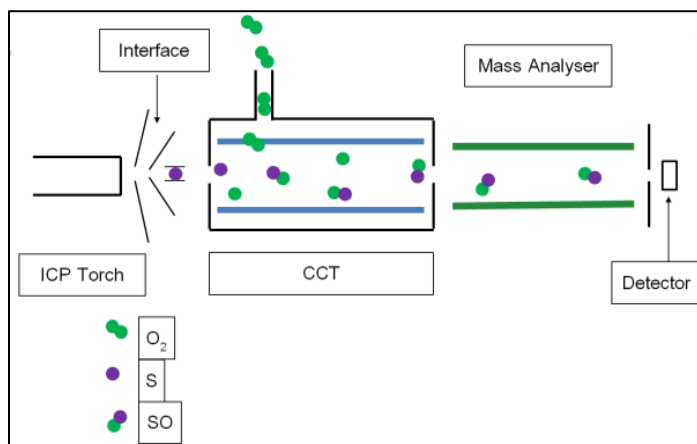


Figure 8: Collision cell, analyte, reaction gas and new formed compound

1.5. Inductively Coupled Plasma Optical Emission Spectrometry (ICP-OES)

Another widely used technique for elemental analysis is inductively coupled plasma optical emission spectrometry.

As mentioned before, the similarities between the ICP-OES and the ICP-MS are present until the analytes are within the plasma. For information about built-up, sample introduction and plasma conditions see Chapter 1.3, 1.4.1 and 1.4.2. When the analyte reaches the plasma, the vaporization-atomization-excitation takes place. Due to the relapse of electrons from the excited state to the ground state, the atoms emit radiation. This radiation is analyzed in an ICP-OES. Atom lines are most intense for elements with high ionization potentials and the alkali metals.²⁸

²⁸ (Olesik, 1991)

Depending on the element and the plasma temperature the intensity of the radiation varies. Because of that, optimal instrument settings have to be tested for the elements being analyzed. Meaning that if using a multielement method, compromises have to be made, since the parameters are used for all the elements analyzed with this method. The emitted radiation enters into the optical system via the ceramic cone next to the plasma. To remove fumes and dust, a purging gas streams vertical to the optical axis. For quantitative and qualitative information from the radiation, it has to be separated into its wavelengths. This is done by a polychromator, consisting of optics (grating, prism) and a detector or with a so called echelle system. An echelle system consists of a grating and a prism, exit slit and a CCT detector. First the radiation hits the grating, being dispersed and the originated spectrum is projected onto the prism. There the radiation is dispersed once more, resulting in a 2D plot that is projected onto a CCD detector. This allows simultaneous multielement analysis. From the wavelength qualitative information is received, the measured intensity provides quantitative information.²⁹

Important for an ICP-OES instrument is the wavelength range, ideally reaching from 120 to 770 nm. Most useful spectral lines for nonmetals (Cl, Br, S) are located in the UV-range, whilst alkali metals (Li, Na, K) are detected at wavelengths over 500 nm. Measuring in the UV-range comes with the disadvantage that oxygen absorbs UV-light. In order to be able to detect emission in the UV-range the instrument has to be purged with a protective gas, such as argon or nitrogen or operated under vacuum. One of the major advantages against ICP-MS instrument is that the ICP-OES is cheaper and easier to operate, as well as the occurrence of less spectral interferences.

When analyzing sulfur with ICP-OES, one big advantage in contrast to ICP-MS measurements is, there are barely any spectral interferences for sulfur. But excitation of sulfur is difficult, leading to low sensitivity. To enhance sensitivity of ICP-OES analysis, improved sample introduction system is of advantage.

Apex E is an additional, more efficient sample introduction system that can be coupled with either ICP-MS or ICP-OES. It increases the sensitivity because it separates the analytes from their matrices, reducing the plasma load by reducing solvent amount and allowing more analyte to reach the plasma. This leads to better excitation and higher sensitivity. Apex E is used for liquid samples. Via a peristaltic pump the liquid samples are transported into the Apex, where the sample is

²⁹ (Nischkauer, 2011)

nebulized and the originated aerosol is carried into a heated, cyclone formed spray chamber. Because of the heating of the aerosol, the solvent vaporizes. From there the small aerosol drops reach a three-part Peltier-cooled desolvation-system where the solvent condenses. Because of the condensation, the solvent is separated from the sample, allowing only the analytes to reach the plasma. The sensitivity increases 6- to 10 times³⁰.

In this work the Apex E was only used in combination with the ICP-OES.

For liquid samples the most common way of quantification is external quantification. Meaning standard solutions with known analyte concentration are measured, leading to a calibration curve and a calibration equation. With that equation, sample concentrations can be calculated. To compensate instrumental drift and matrix effects, internal standards can be added.

1.6. Time of Flight-Secondary Ion Mass Spectrometry (TOF-SIMS)

SIMS is an analytical method for mainly solid samples that allows the analysis of the atomic and molecular composition of 1 to 3 monolayers. Advantages of the instrument are all elements in the periodic table are detectable as well as high lateral resolution and isotope sensitivity. LODs down to $\mu\text{g}/\text{kg}$ can be derived.

Primary ions (e.g. Bi^+ , Ga^+ , Au^+) are shot on the sample surface and from there secondary particles, such as electrons, atoms and ions, are emitted. The primary ions bombarding onto sample surface have high energy (1-25 keV). This energy is transferred to sample surface atoms through billiard-ball-type collision. The secondary ions that are generated are extracted by a TOF mass analyzer. There they are separated according their m/z ratio.³¹

³⁰ (<http://www.icpms.com/pdf/ApexE-ESI.pdf>)

³¹ (Fugger, 2014)

2. Experimental

This chapter gives an overview over the instruments and chemicals that were used for this work, as well as it sample preparation is described.

2.1. Samples and preparation

During this master's thesis 8 different copper wafers were analyzed. Four different additives were used for the manufacturing process (one additive per wafer) and four of the wafers had been tempered at 300°C after the electroplating process. Sample identification is listed in Table 2.

Table 2: Sample identification

| non-tempered wafer | Tempered wafer |
|--------------------|----------------|
| E1 | E1t |
| E2 | E2t |
| E3 | E3t |
| E4 | E4t |

Wafers for analysis were round with a diameter of 20 cm. For measurements the wafers were first cut into quarters with a diamond cutter. For digestion pieces, around 1 cm x 1 cm were then cut. In the pictures Figure 9 to Figure 11 cutting process is shown.



Figure 9: Halv copper wafer

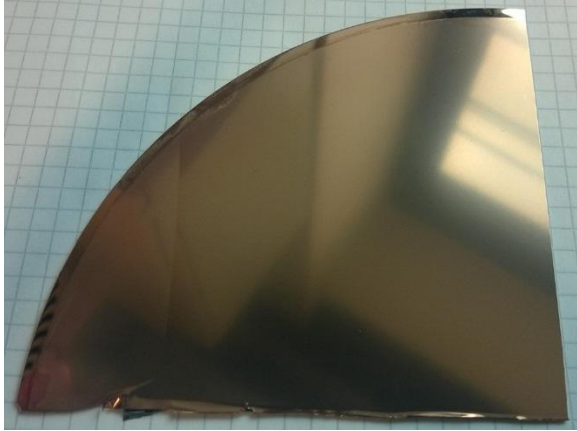


Figure 10: Quarter copper wafer

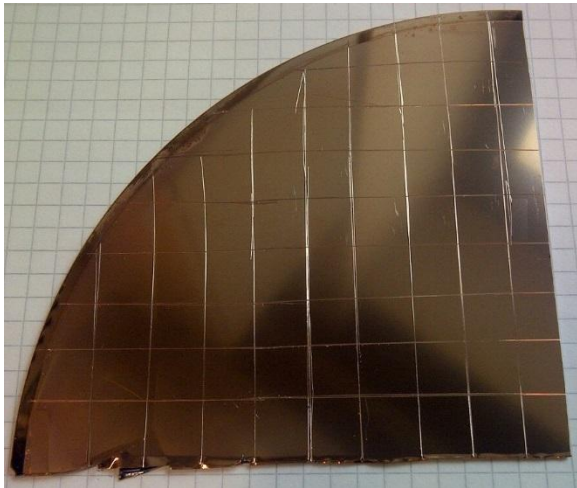


Figure 11: Quarter copper wafer, scratched

2.1. Instrumentation

For analysis a quadrupole ICP-MS (iCAP Q, ThermoFisher Scientific) was used. For liquid sample analysis the instrument was equipped with a concentric quartz glass nebulizer and a peltier cooled spray chamber. For liquid sample introduction the iCAP Q was coupled with an ESI SC-2DXS auto-sampler and a FAST AA sample introduction system (Elemental Scientific, Inc. (ESI)). Software for data acquisition, Qtegra software, was provided with the instrument. The instrument is shown in Figure 12.



32

Figure 12: ThermoFisher Scientific iCAP Q; ICP-MS instrumentation for performed experiments

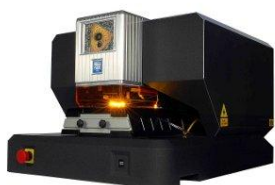
Using a tuning solution (Tune B iCAP Q, Ba, Bi Ce, Co, In, Li, U each 1.0 µg/L in 2% HNO₃ + 0.5% HCl, ThermoFisher Scientific) instrument parameters were optimized before each analysis, for maximum ¹¹⁵In- and minimum ¹⁴⁰Ce ¹⁶O/¹⁴⁰Ce signal ratio.

³² <http://www.thermoscientific.com/content/tfs/en/product/icap-q-icp-ms.html>

Table 3: Measurement parameters of iCAP Q, ICP-MS

| Parameter | Unit | Measurement settings | Measurement settings | Measurement settings |
|---------------------|-------|---|---|---|
| | | Liquid, Standard-mode | Liquid, CCT-mode | Laser, Laser-mode |
| Auxiliary gas flow | L/min | 0.80 | 0.80 | 0.80 |
| Coolant gas flow | L/min | 13.0 | 14.0 | 14.0 |
| Nebulizer gas flow | L/min | 0.98 | 0.98 | 0.80 |
| Collision gas flow | L/min | 0.00 | 1.96 | 0.00 |
| Dwell time/ isotope | s | 0.01 | 0.01 | 0.01 |
| RF power | W | 1550 | 1550 | 1550 |
| Pole bias | V | -1.00 | -12.0 | -1.00 |
| CCT bias | V | -2.00 | -5.60 | -2.00 |
| Cones | - | Ni | Ni | Ni |
| Measured isotopes | - | ³² S, ³⁴ S, ¹¹⁵ In | ³² S, ³⁴ S, ¹¹⁵ In | ³² S, ³⁴ S, ¹²³ Sb |

The laser ablation system (New Wave 213, ESI, see Figure 13) used for solid samples was connected to the iCAP Q via tubing. A frequency quintupled 213 nm Nd:YAG laser is built-in into the New Wave 213. The ablation cell used in this work was specially build, made of aluminum, to avoid plastic, which could contain sulfur. The ablation cup was kept directly over the ablated spot, to ensure a rapid and constant washout behavior. During all laser measurements dry plasma conditions were applied.



33

Figure 13: New Wave 213 ESI, Laser instrumentation used for performed experiments

Laser settings (laser beam diameter, repetition rate, laser output, scan speed and ablation time) are listed in Table 4. These settings were optimized using a self-manufactured pellet, described in

³³ <http://www2.le.ac.uk/departments/geology/analytical/images/213NWRThreeQuarterView.jpg/view>

the next chapter, 2.2. Measurement parameters regarding the ICP-MS and ICP-OES instrumentation were optimized using a reference material, NIST 612 trace metals in glass standard (National Institute of Standards and Technologies) for maximum ^{115}In signal before every experiment. For this standard laser settings were applied, see Table 4.

Table 4: Laser parameters

| Parameter | Unit | Standard settings | Pre-ablation settings | Measurement settings |
|---------------------|-----------------|-------------------|-----------------------|----------------------|
| Laser beam diameter | μm | 80 | 200 | 200 |
| Repetition rate | Hz | 10 | 10 | 10 |
| Output | % | 70 | 95 | 40 |
| Scan speed | $\mu\text{m/s}$ | 5 | 150 | 150 |
| Carrier gas flow | L/min | 0.75 | 0.75 | 0.75 |

Ablation patterns are shown in Figure 14.

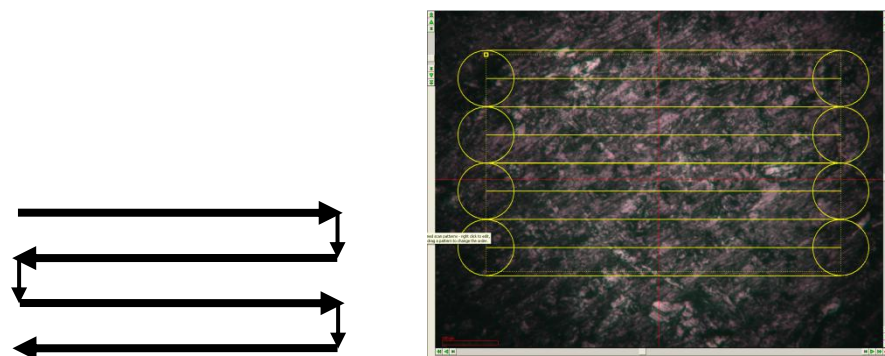


Figure 14: Ablation pattern

For calibration 5 patterns per pellet were ablated.

For calculations, several (5 or more, depending on measurement) regions (see green areas in Figure 15) were placed for each pattern. Gas-blank was subtracted for each region and the average of these regions was calculated. After that, average of the average of the 5 ablated patterns was calculated and used for the calibration. In Figure 15 a time-scan of a LA-ICP-MS measurement is shown. Sample is hit by laser between 21 and 51 seconds. During this time increased signal intensity for analyzed elements can be observed.

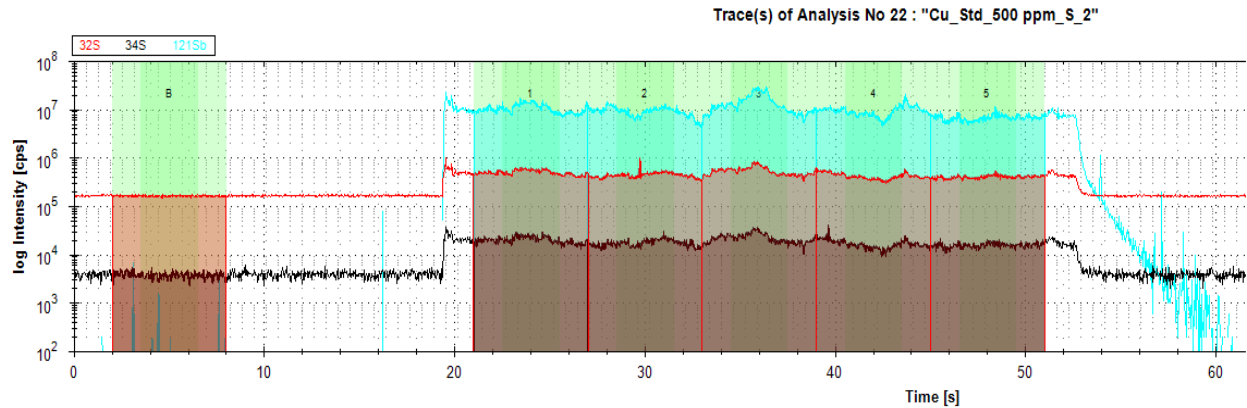


Figure 15: Time-scan, LA-ICP-MS measurement, Blank- and region areas

The ICP-OES used in this work is an iCAP 600 Series (ThermoFisher Scientific), see Figure 16. For liquid sample measurements and introduction it was coupled with the APEX E (ESI) and an ASX-520 autosampler (CETAC Technologies). Sample introduction into the plasma was carried out with a concentric spray chamber and a 1.5 mm quartz glass torch. Optimized measurement settings for the instrument were tested with a 100 ppb sulfur standard solution, matrix-matched in a 1 g/L copper solution. These settings are listed in Table 5.



34

Figure 16: ThermoFisher Scientific iCAP 6000; ICP-OES instrumentation for performed experiments

³⁴ <http://em-1.stanford.edu/EquipmentList.htm>

Table 5: OES measurement parameters

| Parameter | Unit | Measurement settings | |
|-----------------------|-------|-----------------------------------|-----------------------------------|
| | | Liquid | Laser |
| Flush pump rate | rpm | 20 | |
| Analysis pump rate | rpm | 20 | |
| RF-Power | W | 1450 | |
| Radial viewing height | mm | 9.0 | |
| Nebulizer gas flow | L/min | 0.75 | |
| Auxiliary gas flow | L/min | 0.8 | |
| Coolant gas flow | L/min | 12 | |
| Carrier gas flow | L/min | 0.00 | 0.50 |
| Measured wavelengths | nm | S: 180,7; 182,0; Sb: 206,8; 217,5 | S: 180,7; 182,0; Sb: 206,8; 217,5 |

For dilution of liquid sample bi-distilled water was generated by a water distillation machine (GFL 2104, Gesellschaft für Labortechnik).

2.2. Preparation of Pellets

For sulfur quantification using LA reference material had to be manufactured. As mentioned in 1.2, matrix effects occur when ablating different materials due to different ablation and absorption. Several reference materials with certified copper values are available, though non with a copper matrix. Therefore reference material had to be produced in-house.

First tests were carried out mixing copper powder (Cu) and antimony sulfide (Sb_2S_3). This did not result in a homogenous mixture, therefore copper oxide powder (CuO) was added to the copper powder and antimony sulfide. Several mixtures were composed to analyze the homogeneity of the powder mixtures. The compositions are listed in Table 6. To optimize the mixing procedure, 10 respectively 30 ceramic spheres were added to the powder mixture, to see if the quantity of ceramic spheres has an influence on the homogeneity.

Table 6: Pellet composition, rounded, all contain 100 ppm sulfur

| Pellet | Cu [%] | CuO [%] |
|------------------|--------|---------|
| 10/30 Spheres _1 | 90 | 10 |
| 10/30 Spheres _2 | 80 | 20 |
| 10/30 Spheres _3 | 60 | 40 |
| 10/30 Spheres _4 | 50 | 50 |
| 10/30 Spheres _5 | 40 | 60 |
| 10/30 Spheres _6 | 20 | 80 |
| 10/30 Spheres _7 | 0 | 100 |

In a first step 0.05 g of Sb_2S_3 powder were mixed with 0.45 g of CuO powder. The powders were weight out into a 2 mL Eppendorf vial. These vials were then placed in an ultrasonic swing mill (MM400, Retsch). Mixing process was performed at 20 sec^{-1} for 15 minutes. The content of the vials was emptied into a weighing pan and homogenized. After that they were transferred into the Eppendorf vial again and mixed for 15 more minutes at 20 sec^{-1} .

For the second step, 0.05 g of this Sb_2S_3/CuO powder mixture was weight out with the respective composition of Cu and CuO powders into an Eppendorf vial. The mixing process was equal to the one described in step one.

1 g of each powder mixture was then grouted with a pneumatic press, 10 tons, for 30 seconds. Resulting in a pellet with 13 mm diameter and about 1 mm in height. All pellets had a sulfur concentration of ~1000 ppm.

After measurement of these pellets, based on the results, the most homogeneous composition was determined and new pellets were manufactured. Six pellets were produced, with resulting sulfur concentrations of 0, 50, 100, 250, 500 and 750 ppm. Those pellets were used to generate a calibration. The mixing process was carried out identically as for the manufacturing of the first pellets, but different amounts of the Sb_2S_3/CuO powder mixture were weight out in the second step, resulting in the above-named concentrations.

2.3. Digestion of Copper Wafers

The cut wafer pieces were peeled from the silicon layer of the wafer and placed in PE-tubes and 250 μL HNO_3 conc. were added. Samples of Wafer E4t were digested in 125 μL HNO_3 conc. and 125 μL H_2O_2 . After dissolution of the copper layer the sample was diluted with 1750 μl 1% HCl (HCl conc. diluted with bi-dest. water).

1 mL from this solution was pipetted into PE-tubes and diluted with 8 mL 1% HCl (HCl conc. diluted with bi-dest. water). For ICP-MS measurements 90 μL of a 100 ppb indium (In) stock solution were added as internal standard. Measurements carried out with ICP-OES needed a higher indium concentration, so 100 μL of a 100 ppm In stock solution were added. Internal standard was added to correct instrument induced effects, such as instrumental drifts etc. Chemicals used for digestion process are listed in Table 7.

Table 7: Chemicals used for copper wafer digestion

| Chemical | Name | Annex | Company |
|-----------------------|-----------------------------------|--|---------|
| HNO_3 | Nitric acid 65% | Emsure [®] ISO | Merck |
| HCl | Hypochlorite acid fuming 37% | Emsure [®] ACS, ISO, Reag. Ph Eur | Merck |
| Indium stock solution | Indium ICP standard, 1000 mg/L In | Certipure [®] | Merck |

2.4. Preparation of Standards

2.4.1. Standards for Calibration

Standards were prepared before each measurement. Depending on the samples to be analyzed, different concentrations were manufactured. Lowest concentration standard was always 0 ppb (blank).

For ICP-MS analysis a 1 g/L sulfur stock solution was prepared. Sodium sulfate (Na_2SO_4) was dried at 70°C over night and then weight in and diluted with 1% HNO_3 (HNO_3 conc. diluted with bi-dest. water), resolving in a 1 g/L sulfur stock solution. From that solution calibration standards were prepared before each measurement, by dilution with 1% HCl (HCl conc. diluted with bi-dest. water).

Standards for ICP-OES analysis were prepared from an ICP-MS calibration standard solution, diluted with 1% HCl (HCl conc. diluted with bi-dest. water).

Table 8: Chemicals used for calibration standards

| Chemical | Name | Annex | Company |
|---------------------------------|--|--|----------------|
| Na ₂ SO ₄ | Sodium sulfate anhydrous GR for analysis | ACS, ISO pro analysis | Merck |
| ICP-MS standard | ICP-MS Calibration standard 4, 10 mg/L | Prolabo [®] | VWR |
| HCl | Hypochlorite acid fuming 37% | Emsure [®] ACS, ISO, Reag. Ph Eur | Merck |
| HNO ₃ | Nitric acid 65% | Emsure [®] ISO | Merck |

2.4.2. Matrix Matched Calibration

When measuring liquid samples, matrix effects can occur. This means, that plasma condition can vary when samples with different matrices are introduced. These matrix effects are mainly a result of differences in viscosity, density and surface tension between different matrices, resulting in different nebulization and plasma-entry of the sample. To avoid this, calibration can be matched to the matrix of the samples to be analyzed.

MMC standards were prepared as the standards in 2.4.1, but instead of using 1% HCl (HCl conc. diluted with bi-dest. water) for dilution of the sulfur standard, a 1 g/L Cu-solution was made. For that 2.1158 g CuCl₂ were weight out and diluted in 1 liter 1% HCl (HCl conc. diluted with bi-dest. water).

Table 9: Chemicals used for matrix matched calibration

| Chemical | Name | Annex | Company |
|--|------------------------------------|--|----------------|
| CuCl ₂ *xH ₂ O (x~2) | Copper(II)chloride hydrate 99,999% | Puratronic [®] | Alfa Aesar |
| HCl | Hypochlorite acid fuming 37% | Emsure [®] ACS, ISO, Reag. Ph Eur | Merck |

2.5. TOF-SIMS

Depth profiles were analyzed for all wafers. For this a TOF-SIMS 5, ION-TOF GmbH, was used.

For depth profiling the High Current Bunched Mode (HCBU) with high mass resolution and low lateral resolution was used. An area of 50 µm x 50 µm was investigated using a raster of 128 x

128 measurement points. A raster of 250 μm x 250 μm was used for the 2 kV caesium sputter gun. Negative secondary ions were analyzed.³⁵



36

Figure 17: ION-TOF GmbH, TOF-SIMS 5

³⁵ (Larisegger, 2014)

³⁶ <http://www.iontofusa.com/news.htm>

3. Results and Discussion

All limits of detection in this chapter were calculated using following equation:

$$\frac{(bl_{av} - 3 * \sigma) - d}{k}$$

| | |
|----------------------|--|
| bl _{av} ... | Average of blank measurements |
| σ... | Standard deviation of blank measurements |
| d... | Intercept of calibration line |
| k... | Slope of calibration line |

3.1. Method Development for Liquid Measurements

3.1.1. ICP-MS, Comparison Standard-mode vs CCT-mode

First measurements for comparison of detecting sulfur as ³²S in standard mode versus detection of ¹⁶O ³²S, using the reaction cell, were carried out. For that a calibration was prepared, as described in 2.4.1, and measured in standard- and CCT-mode. The results of this measurement are illustrated in Figure 18.

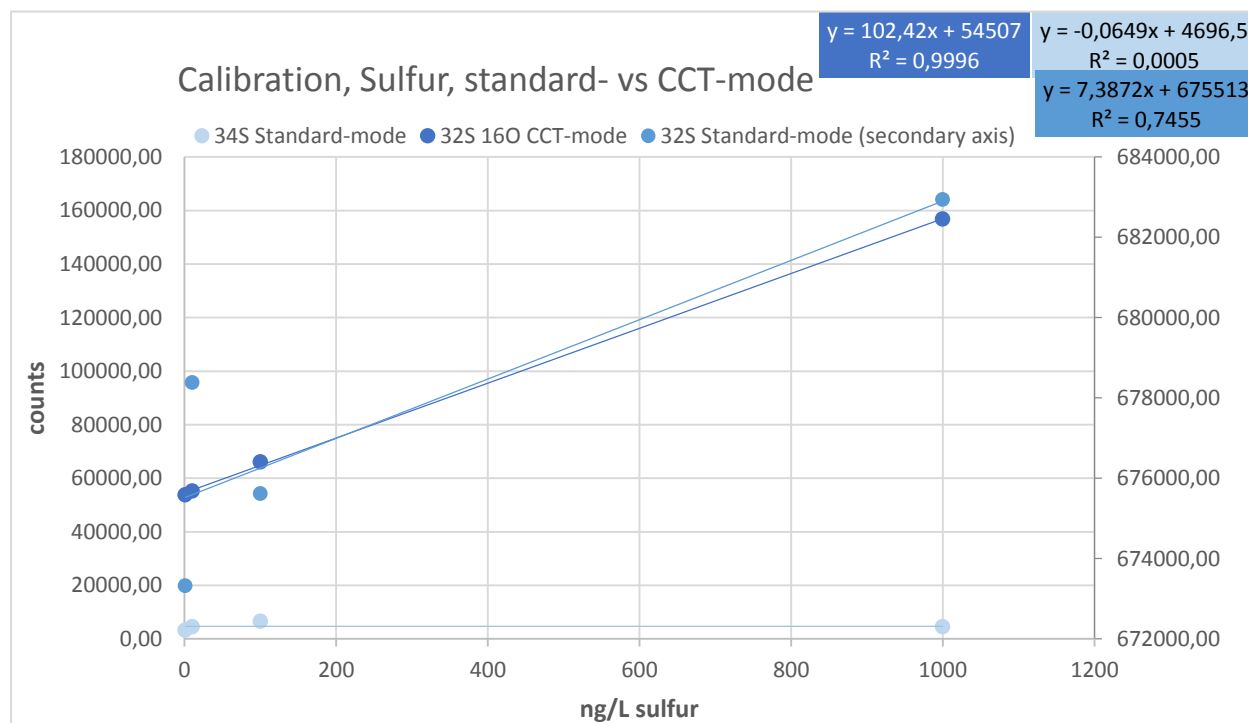


Figure 18: ICP-MS measurement, Comparison calibration standard- vs CCT-mode

For all three measured sulfur signals the slope does not go through point of origin. This resolves from high underground signals. The high background signal is produced from different sources. Main reasons are the O_2 forming from liquids, the fact that used reagents and water are not completely sulfur free and because of tubes in the ICP-instruments that are made of polymers and may contain sulfur.

Analysis on sulfur isotope ^{34}S were not successful due to the fact that sulfur concentration from the sample solution does not lead to an increased signal, resulting in no slope of the calibration. ^{32}S calibration was not successful either and it is shown that only measurements using the reaction cell, detecting sulfur as $^{16}O^{32}S$, result in a linear with an acceptable slope.

Further liquid ICP-MS measurements were carried out in CCT-mode. Further measurements were carried out to obtain lowest possible LOD's. Calibration with sulfur-standards between 0 to 10 ppb sulfur resulted in LOD of 1.85 ppb sulfur on ^{32}S .

3.1.2. ICP-OES

To gain lowest possible LOD's, measurement parameters for ICP-OES instrument, coupled with APEX E, were tested using a 100 $\mu\text{g/L}$ sulfur standard solution. For optimized parameters see Table 5. Calibration between 0 and 50 ppb was analyzed. Results are shown in Figure 19. Same as in chapter 3.1.1 calibration does not start at point of origin. Limit of detection for sulfur was 5.34 ppb.

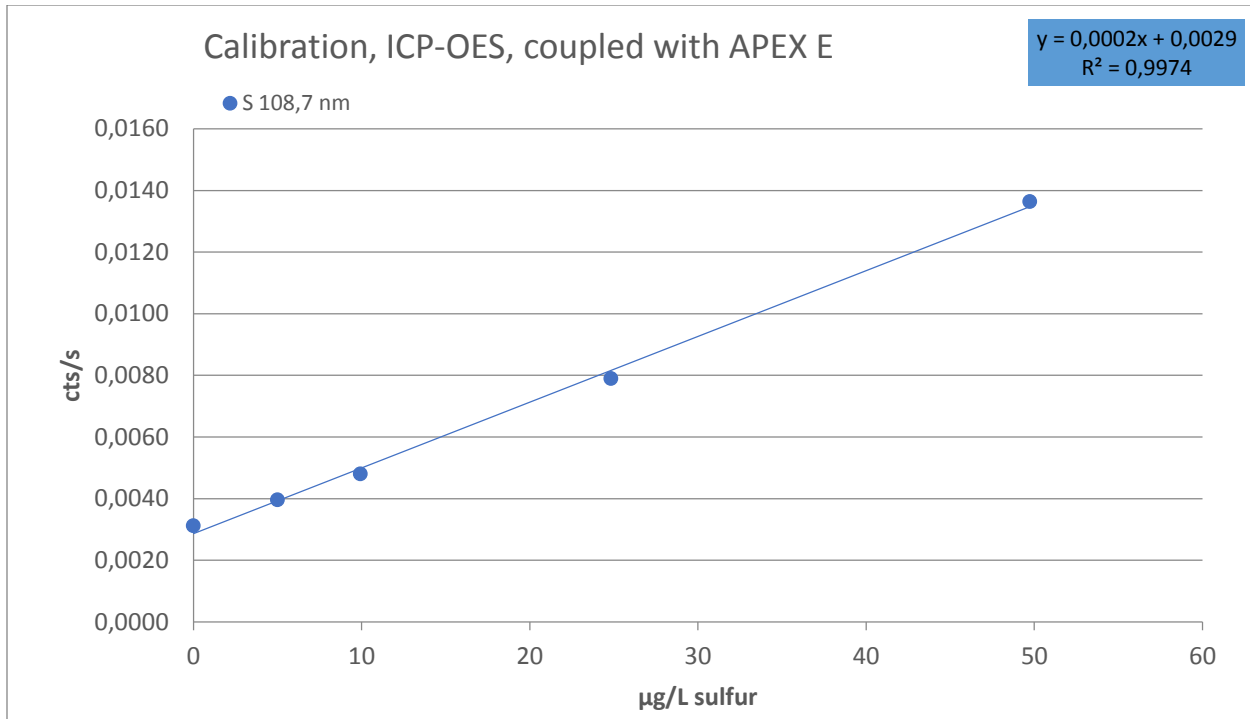


Figure 19: ICP-OES-measurement, coupled with APEX E, first calibration

Based on results obtained with ICP-MS and ICP-OES it can be concluded that measurement of sulfur is possible with ICP-instruments, though it is not as effortless as with other analytical methods, due to high underground signals and problem of sulfur-free chemicals for preparation of standards and digestion of solid samples. Therefore analysis of solid samples holds big advantages.

3.2. Method Development for Solid Measurements

3.2.1. Pellets, Preparation of Sulfur Containing Copper Standards for LA Calibration Measurements

To obtain best possible results first measurements for optimized laser-measurement-parameters were carried out. In Table 10 influence of laser beam diameter is shown.

Antimony was measured to see if a homogeneous distribution could be found for this element as well. Also, to know if sulfur and antimony peaks match, meaning that if a sulfur peak is gained, an antimony peak should be seen as well. Pictures of this are shown in 3.2.3.

Table 10: LA-ICP_MS measurement, Optimization of laser beam diameter for ³⁴S and ¹²³Sb, Region Area

| Laser beam diameter | Average [cts] | Standard deviation [cts] | RSD [%] |
|-------------------------|---------------|--------------------------|---------|
| ³⁴S | | | |
| 100 μm | 112921 | 110822 | 98 |
| 150 μm | 136902 | 115252 | 84 |
| 200 μm | 149687 | 72799 | 49 |
| 250 μm | 211802 | 52850 | 25 |
| ¹²³Sb | | | |
| 100 μm | 80217393 | 72748721 | 91 |
| 150 μm | 106089219 | 84199132 | 79 |
| 200 μm | 102045475 | 55621825 | 55 |
| 250 μm | 189947324 | 96994027 | 51 |

For further analysis laser beam diameter 200 μm was chosen. Though RSD is lower with 250 μm diameters, using 200 μm diameters allowed the application of higher laser output, resulting in deeper ablation. This is important for wafer analysis, see chapter 3.3.2.

After optimized laser parameters, see Table 4, first pellets, as standards for calibration and therefore also sulfur quantification, were manufactured. All 14 produced pellets had a resulting concentration of 1000 ppm sulfur, for pellet compositions see Table 6. To prevent contaminations in the ICP-MS instrument, from high sulfur concentrations, the pellets were measured using LA-ICP-OES. Before carrying out measurements, both LA-chamber as well as ICP-OES were purged with helium resp. argon for over two hours. This was done before every analysis using ICP-OES. Results of those measurements can be seen in Table 18, Table 19 and Figure 20.

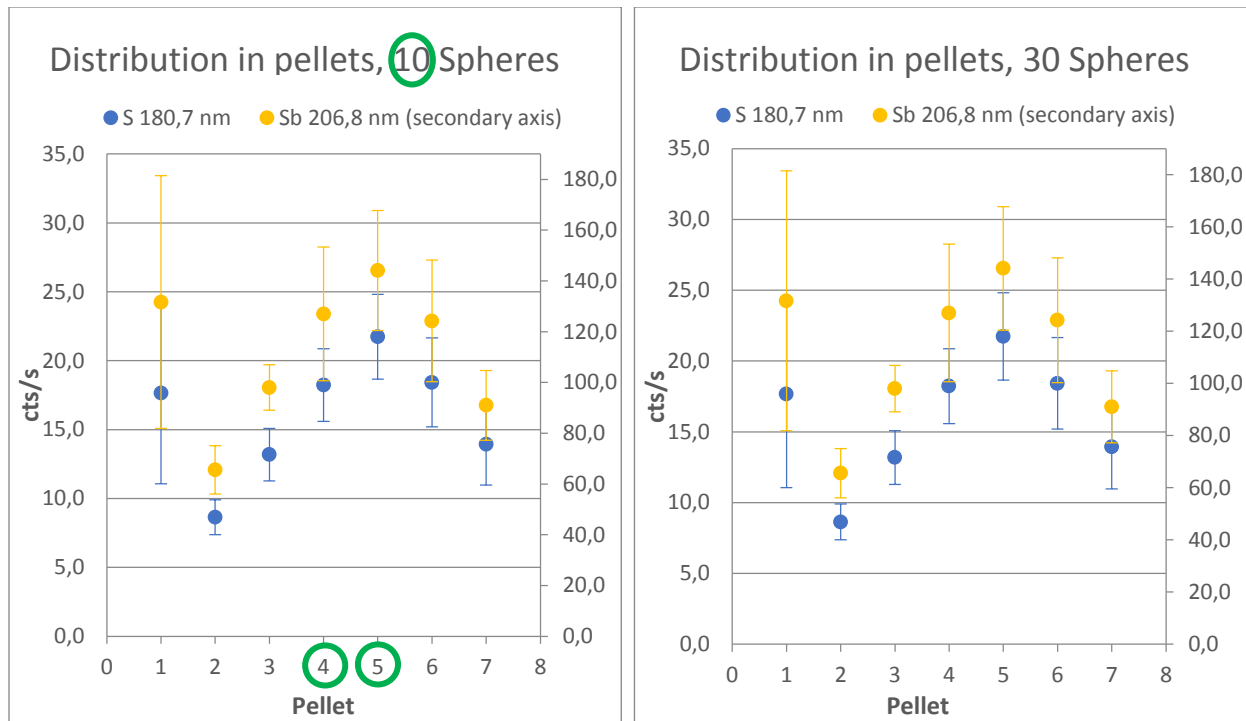


Figure 20: LA-ICP-OES measurement, Distribution of sulfur and antimony in pellets, prepared with 10 resp. 30 spheres, Numbers see Table 18 and Table 19

Most homogeneous distributions of sulfur and antimony were derived for compositions 4 and 5 for pellets that were mixed with 10 ceramic spheres.

New pellets with those two compositions were manufactured with resulting sulfur concentrations of 0, 500 and 1000 ppm sulfur. Those were analyzed to determine if one of the two chosen compositions results in a more linear and homogeneous linear slope. Results of LA-ICP-OES measurements are shown in Figure 21. More homogeneous distribution was derived for pellets with composition 4.

For the manufacturing of calibration standards composition 4 (50% Cu- and 50%CuO-powder) with addition of 10 ceramic spheres was chosen. 6 standards with sulfur concentrations of 0, 50, 100, 250, 500 and 750 ppm were produced.

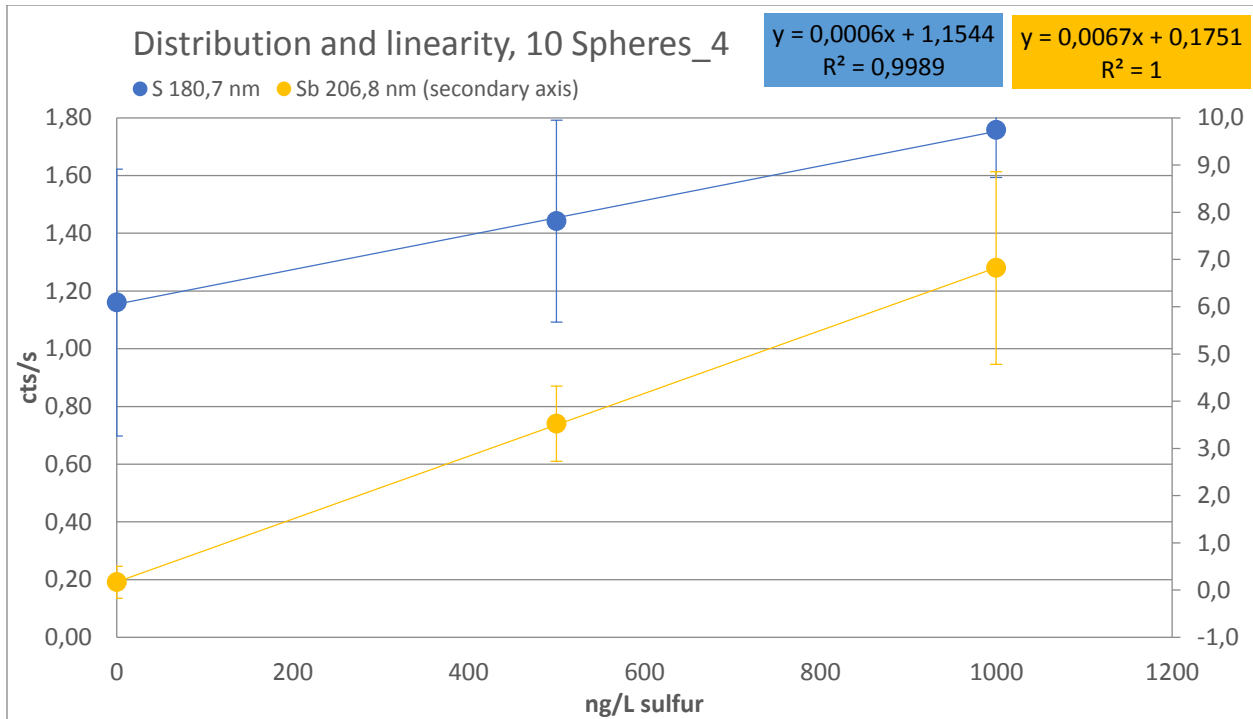


Figure 21: LA- ICP-OES measurement, Distribution and linearity of sulfur and antimony in pellet with composition 4

3.2.2. LA-ICP-OES

Manufactured pellets for calibration with composition 4, using 10 ceramic spheres for mixing process were analyzed using LA-ICP-OES. Results can be seen in Table 20 and Figure 22.

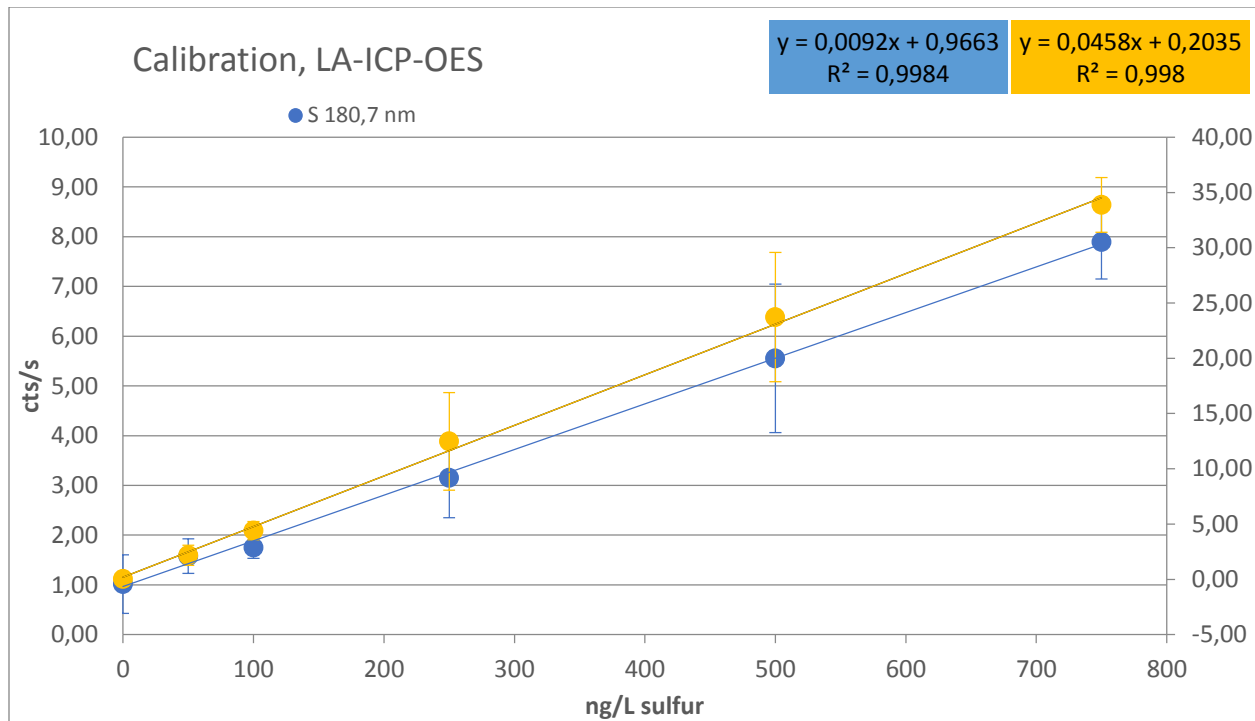


Figure 22: LA-ICP-OES measurement, calibration with pellets, Numbers see Table 20

Linear results with satisfactory slopes were obtained. It can be observed that antimony-calibration derives from point of origin, whereas this is not the case for sulfur-calibration. Reasons for that is that also when analyzing solid samples a sulfur background occurs. This background signal derives from sulfur containing tubes in the ablation chamber.

3.2.3. LA-ICP-MS

After successful analysis of the calibration pellets using LA-ICP-OES it was tested if these results could also be obtained using ICP-MS. Before starting the measurements, the pellets were placed in the ablation chamber of the LA-instrument and purged with helium for two hours to reduce high sulfur background. Gained results are shown in Table 21 and Figure 23.

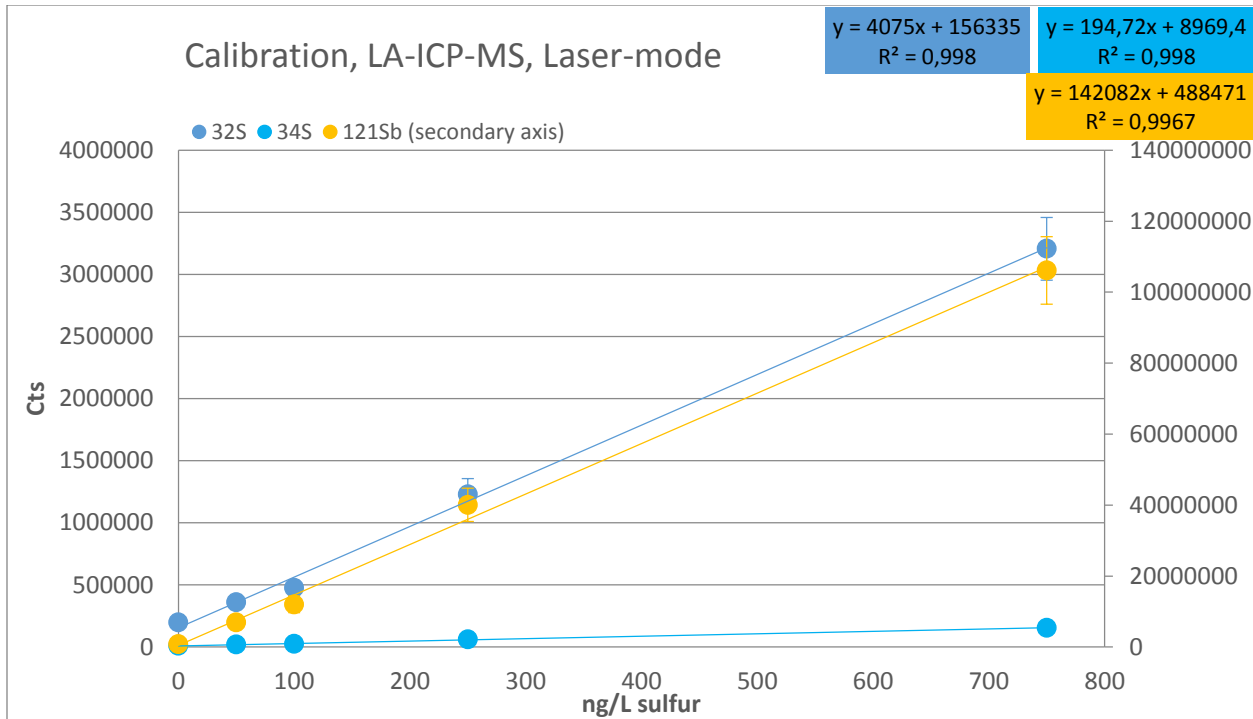


Figure 23: LA-ICP-MS measurement, laser-mode, calibration with pellets, without standard 500 ppm (outlier), for Numbers see Table 21

Due to the fact that oxygen was removed from the ablation chamber because of long purging time it was possible to measure both sulfur isotopes without usage of the reaction cell. Obtained slopes were better for ^{32}S than for ^{34}S , because more counts were gained and therefore measurements of ^{32}S are more accurate. For further measurements only sulfur isotope ^{32}S is shown, due to this fact. Coefficient of determination is satisfactory for all measured isotopes. Relative standard deviation for ^{32}S lies between 5 and 12%.

In Figure 24 to Figure 26 time-scans of LA-ICP-MS measurements of calibration pellets are shown. They show signal progression of the measured scan. It can be observed that even though mixing process was optimized, the pellets are not completely homogenous. However, due to the average being taken over a big sample area a linear correlation can be gained.

Correlation between detected sulfur and antimony signals can be observed. Meaning if sulfur is detected above background level, it derives from Sb_2S_3 . Due to the shown sulfur correlation, to the linear slopes and because this element is not relevant for wafer analysis antimony is not shown in further diagrams and tables.

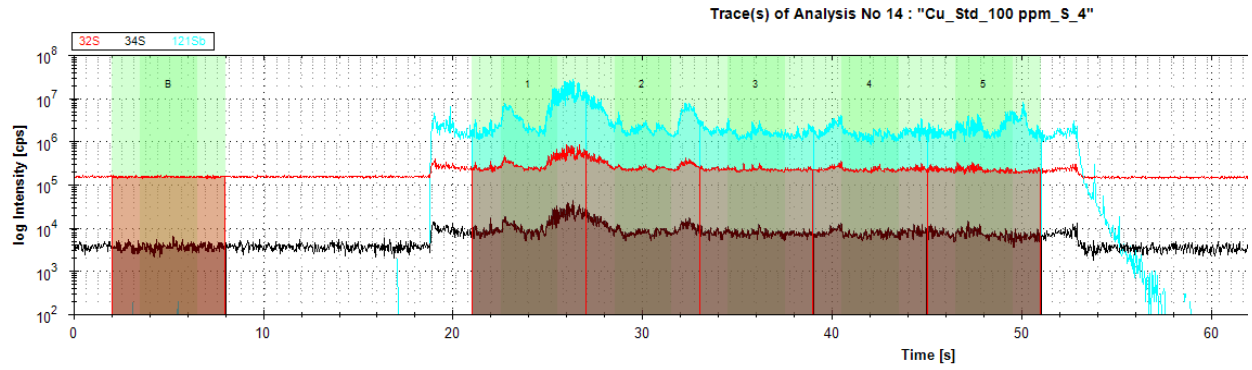


Figure 24: Time-scan of LA-ICP-MS analysis of pellet with 100 ppm sulfur concentration

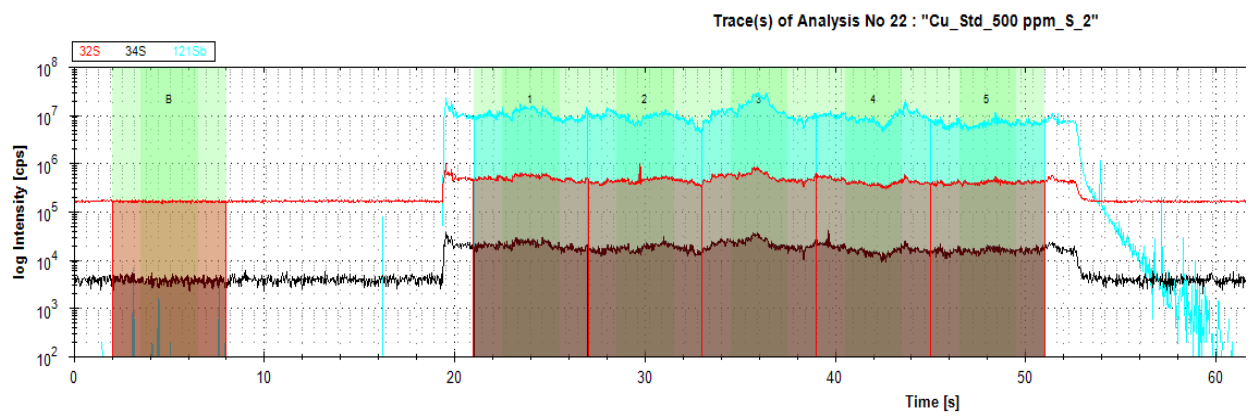


Figure 25: Time-scan of LA-ICP-MS analysis of pellet with 500 ppm sulfur concentration

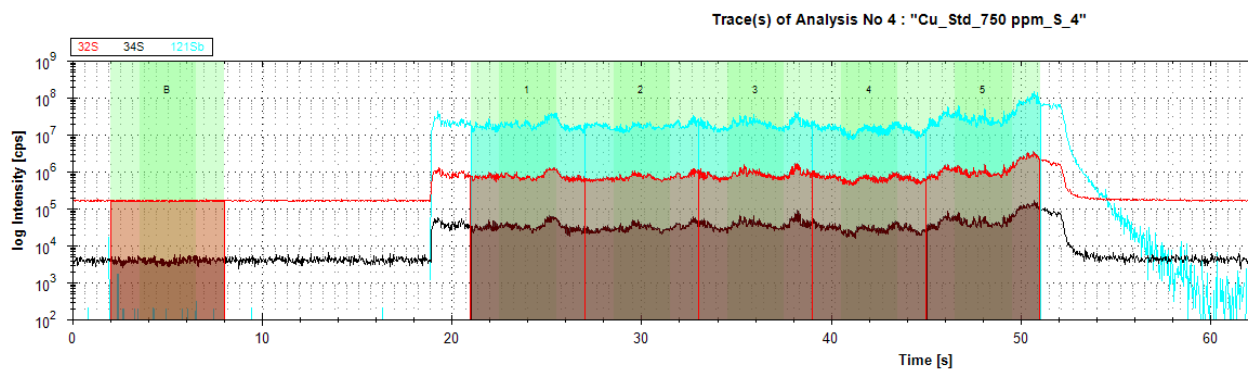


Figure 26: Time-scan of LA-ICP-MS analysis of pellet with 750 ppm sulfur concentration

A comparison between derived LA-ICP-MS and LA-ICP-OES LOD is listed in Table 11. It can be seen, that the LOD derived from MS measurements is a factor 4.4 lower than the one obtained with OES. Therefore the wafers in solid state were only analyzed with LA-ICP-MS.

Table 11: LOD's for calibrations obtained with LA-ICP-OES and LA-ICP-MS

| Instrument | Element measured | ppm |
|------------|------------------|-----|
| LA-ICP-OES | S 180,7 nm | 197 |
| LA-ICP-MS | ³² S | 28 |

3.3. Results Wafer

As described in 2.3 the copper layer of the wafer was peeled off for digestion process. However, this was only possible for wafers E1-E3 and E1t-E3t, not for E4 and E4t. In Figure 27 a picture of E1 and E4 is shown. Wafer E4 and E4t look very different from wafers E1-E3 and E1t-E3t. Their surface is not polished and light-reflecting. Also regions with different colors can be seen. Those facts suggest that different results may be expected.

The copper layer was non-peelable, therefore the wafer was broken into pieces. Those pieces were placed in a tube with acid for digestion and after dilution the remaining silicone layer was dried and weight out to determinate weight of the copper layer that was dissolved and analyzed.

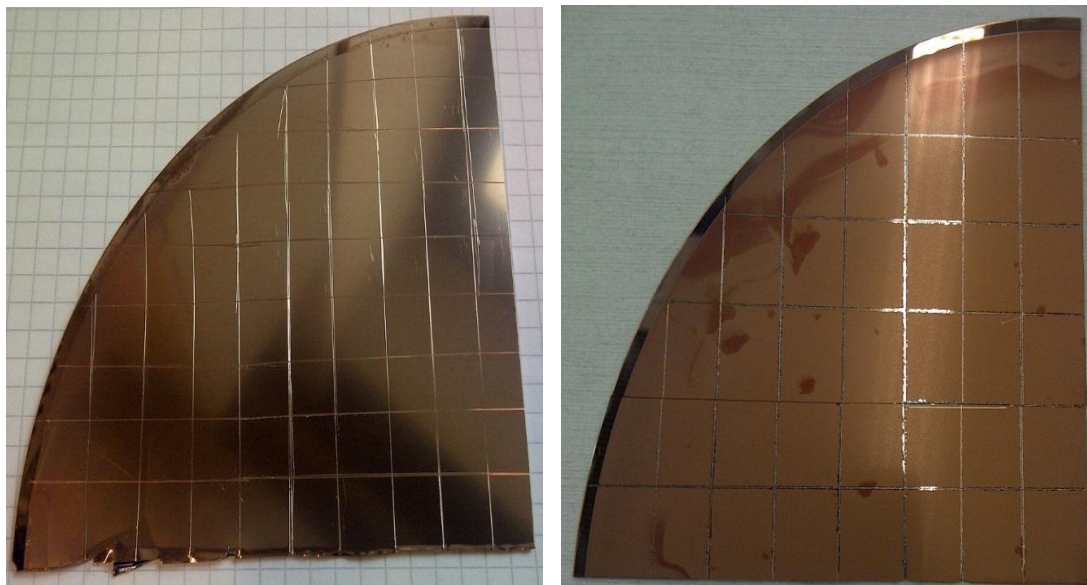


Figure 27: Wafer E1 and E4, comparison

Color scale used for all figures and tables in this chapter is shown in Figure 28.



Figure 28: Color scale used in chapter 3

3.3.1. Liquid

3.3.1.1. ICP-MS

Based on results derived from ICP-MS liquid analysis, total sulfur concentration in the solid copper layer was calculated for each copper wafer piece. Concentrations are listed as mg/kg (ppm) sulfur in solid.

Liquid analysis of wafer E1 to E4, using ICP-MS with reactive cell, lead to results listed in Figure 29 and Figure 30. Results were calculated from measurement of $^{16}\text{O}^{32}\text{S}$ on $m/z=48$. Sulfur concentration in solid sample are homogeneous for all wafers, variation can derive from uncertainty of measurement.

LOD was 8.75 $\mu\text{g/L}$ (ppb). Blank values were below LOD and measured sulfur signals on $m/z=48$ were between 3000 to 5000 $\mu\text{g/L}$ (ppb).

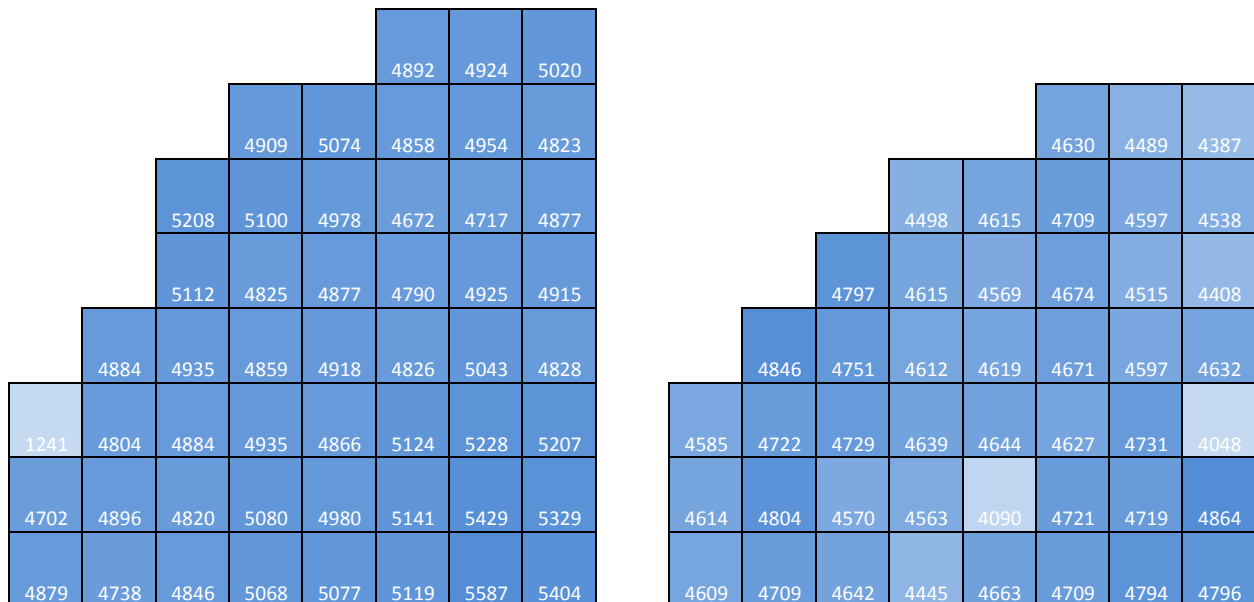


Figure 29: ICP-MS with reaction cell analysis, Wafer E1 and E2, [mg/kg] sulfur in solid

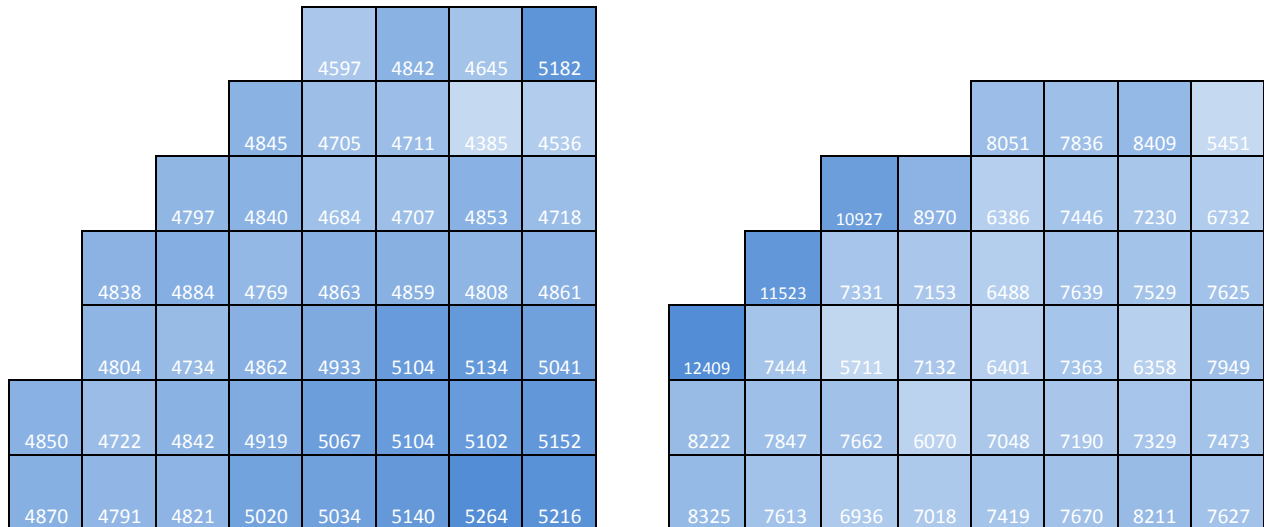


Figure 30: ICP-MS with reaction cell analysis, Wafer E3 and E4, [mg/kg] sulfur in solid

Average sulfur amount for wafers E1 to E3 lay around 4800 mg/kg (ppm), for wafer E4 it was even higher with 7600 mg/kg (ppm). Concentrations in these dimensions were not as expected (few mg/kg (ppm)). Somewhere an error was suspected and more tests were conducted.

After some experiments to determinate isotope ration by measuring $^{16}\text{O}^{32}\text{S}$ and $^{16}\text{O}^{34}\text{S}$ it became clear that obtained counts did not derive from sulfur. After some more experiments it was found that during digestion process of the copper-layer the WTi-barrier-layer partly also was digested. Since $^{16}\text{O}^{32}\text{S}$ is detected on $m/z=48$, where also ^{48}Ti is detected, the high intensities derive from titanium in the sample solution.

Other ways to digest the copper-layer were tried, but none successfully without also digesting the WTi-barrier-layer.

To avoid spectral interferences from oxygen when analyzing sulfur a reactive cell has to be used leading to the formation of $^{16}\text{O}^{32}\text{S}$. Since this molecule is detected on $m/z=48$ the sample solution has to be titanium (^{48}Ti) free. This was not possible for these wafers, therefore wafer-analysis could not be carried out using liquid ICP-MS with reaction cell.

3.3.1.2. ICP-OES

3.3.1.2.1. E1, E1t, E2, E2t, E3, E3t

Solutions analyzed in chapter 3.3.1.1 were used for measurements in this chapter. Analyzing these solutions with ICP-OES resulted in very different sulfur concentrations. All measured sulfur concentrations were below LOD.

For all investigated pieces the LOD of the measurement was referenced to volume of acid and water added and then references to the amount of copper weight-out for digestion, and so a LOD for each solid sample piece was calculated. These values resemble a limit of detection in mg/kg (ppm). LOD for the solid pieces is listed in Figures and tables in this chapter. Deviation between pieces can occur because the size and mass of copper digested was different for the pieces.

Measured LOD for analysis of wafers E1 to E3 LOD was 5.34 µg/L (ppb) and for E1t to E3t LOD was 8.37 µg/L (ppb). Blank values were below LOD.

| | | | | | | | |
|-------|-------|-------|-------|-------|-------|-------|-------|
| | | | | | <12.9 | <9.65 | <7.80 |
| | | | <20.8 | <8.67 | <10.0 | <10.0 | <9.24 |
| | | <16.5 | <10.1 | <9.17 | <8.64 | <8.97 | <8.70 |
| | | <9.16 | <8.59 | <8.08 | <7.38 | <9.40 | <8.55 |
| | <9.26 | <8.17 | <8.10 | <7.96 | <7.15 | <7.62 | <7.48 |
| <7.29 | <5.98 | <6.97 | <7.55 | <7.32 | <7.70 | <8.11 | <7.53 |
| <11.4 | <7.33 | <7.00 | <6.51 | <6.98 | <7.20 | <8.83 | <7.71 |
| <9.48 | <7.14 | <7.45 | <7.83 | <6.93 | <6.65 | <7.24 | <7.76 |

Figure 31: ICP-OES analysis of wafer E1, LOD for solid sample [mg/kg]

Since all obtained concentrations were below LOD and to reduce measurement time, analysis of 10 (resp. 8 for the tempered wafers) samples from each wafer was conducted to see if the sulfur concentrations in these wafers are also below LOD.

Table 12: ICP-OES analysis of Wafer E1t

| Wafer E1t | |
|-----------|---------------------------------|
| | Sulfur content in solid [mg/kg] |
| E1t_1 | <19 |
| E1t_2 | <13 |
| E1t_3 | <13 |
| E1t_4 | <11 |
| E1t_6 | <11 |
| E1t_7 | <11 |
| E1t_8 | <11 |

Table 13: ICP-OES analysis of Wafer E2 and E2t

| Wafer E2 | |
|-----------|---------------------------------|
| | Sulfur content in solid [mg/kg] |
| E2_1 | <6 |
| E2_6 | <7 |
| E2_17 | <8 |
| E2_21 | <6 |
| E2_23 | <8 |
| E2_25 | <8 |
| E2_37 | <7 |
| E2_43 | <26 |
| Wafer E2t | |
| E2t_1 | <9 |
| E2t_2 | <10 |
| E2t_3 | <10 |
| E2t_4 | <12 |
| E2t_5 | <9 |
| E2t_6 | <12 |
| E2t_7 | <10 |
| E2t_8 | <9 |

Table 14: ICP-OES analysis of Wafer E3

| Wafer E3 | |
|-----------|---------------------------------|
| | Sulfur content in solid [mg/kg] |
| E3_2 | <6 |
| E3_6 | <6 |
| E3_11 | <6 |
| E3_13 | <6 |
| E3_19 | <4 |
| E3_25 | <6 |
| E3_28 | <6 |
| E3_33 | <7 |
| E3_36 | <7 |
| E3_41 | <7 |
| Wafer E3t | |
| | Sulfur content in solid [mg/kg] |
| E3t_1 | <21 |
| E3t_2 | <8 |
| E3t_3 | <28 |
| E3t_4 | <16 |
| E3t_5 | <12 |
| E3t_6 | <11 |
| E3t_7 | <14 |
| E3t_8 | <18 |

In Table 12, Table 13 and Table 14 results for wafers E1t, E2, E2t, E3 and E3t are listed. In none of the analyzed copper-layers sulfur concentrations were higher than LOD.

As expected, interferences from titanium, as observed in chapter 3.3.1.1, did not occur during ICP-OES measurements. Concentrations gained from ICP-MS analysis were proven wrong.

3.3.1.2.2. E4 and E4t

LOD for wafer E4 was 35.3 µg/L (ppb) and for E4t LOD was 6.41 µg/L (ppb). Measured blank values were lower than LOD. Measured values for liquid samples varied between 1500 to 2000 µg/L ppb for E4 and around 170 to 200 µg/L ppb for wafer E4t. So for both wafers results significantly higher than LOD were derived. Major differences in sulfur concentrations for these wafers were gained compared to wafers E1 to E3 and E1t to E3t.

Results from liquid analysis were referenced to the volumes of acid and water used during digestion and dilution and then referenced to the amount of copper weight-out. Calculated concentrations of sulfur in solid samples are shown in Table 15 and Figure 32.

| | | | | | | | |
|------|------|------|------|------|------|------|------|
| | | | | 1591 | 1745 | 1767 | 1750 |
| | | 1709 | 1812 | 1835 | | 1878 | 1929 |
| | 1734 | 1620 | 1524 | 1941 | 2059 | 1914 | 1943 |
| 1818 | 1631 | 1802 | 2124 | 1849 | 1886 | 1538 | 1814 |
| 1727 | 1803 | 1951 | 1765 | 1923 | 1803 | 2003 | 1822 |
| 1773 | 1854 | 1774 | 1821 | 1959 | 1789 | 1908 | 1914 |

Figure 32: ICP-OES analysis of E4, [mg/kg] sulfur in solid sample

Table 15: ICP-OES analysis of Wafer E4t, [mg/kg] sulfur in solid sample

| Wafer E4t | S 180,7 nm |
|--------------------------------|------------|
| sulfur in solid sample [mg/kg] | |
| E4t+H2O2_1 | 316 |
| E4t+H2O2_2 | 332 |
| E4t+H2O2_3 | 337 |
| E4t+H2O2_4 | 330 |
| E4t+H2O2_5 | 322 |
| E4t+H2O2_7 | 339 |
| E4t+H2O2_8 | 369 |

Table 16: ICP-OES measurements, Sulfur concentration average of Wafers E4 and E4t

| Wafer | Average [mg/kg] | Standard deviation [mg/kg] | RSD [%] |
|-------|-----------------|----------------------------|---------|
| E4 | 1820 | 129 | 7 |
| E4t | 335 | 17 | 5 |

Sulfur concentrations of wafers E4 and E4t are significantly higher than from wafers E1 to E3 and E1t to E3t. The distribution of sulfur is homogeneous in the quarter that was analyzed. A substantially higher sulfur concentration was derived from wafer E4. This suggests that sulfur evaporates during tempering process.

As described in chapter 3.3, wafers E4 and E4t behaved different than the other wafers. So it can be observed that higher sulfur concentration result in more brittle material.

3.3.2. Solid, LA-ICP-MS

Depending on received concentrations from ICP-OES analysis of wafers E1 to E3 and E1t to E3t it was assumed that LA-ICP-MS analysis would not be possible since derived LODs are higher than LODs gained for liquid analysis using ICP-OES instrumentation. To prove this hypothesis test-shots were conducted. In Figure 33 a time-scan of wafer E1 is shown. It can be observed that no change in signal occurs, no sulfur is detected. Increase of the signal intensity gained for E4t, see Figure 34, was too small for quantification. Therefore only wafer E4 was analyzed.

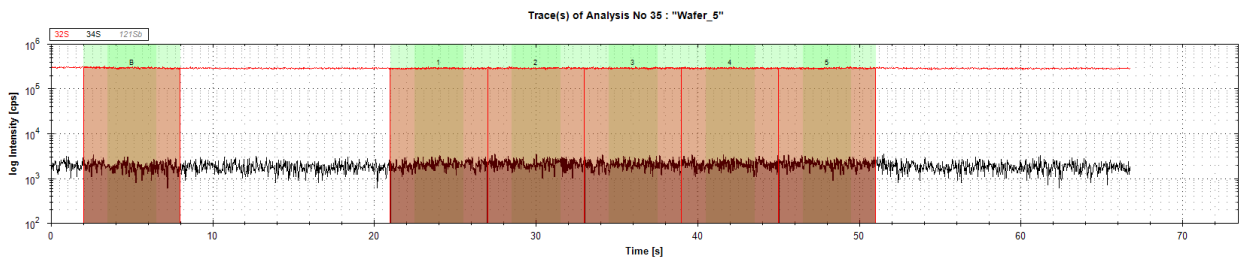


Figure 33: Time-scan of LA-ICP-MS analysis of Wafer E1

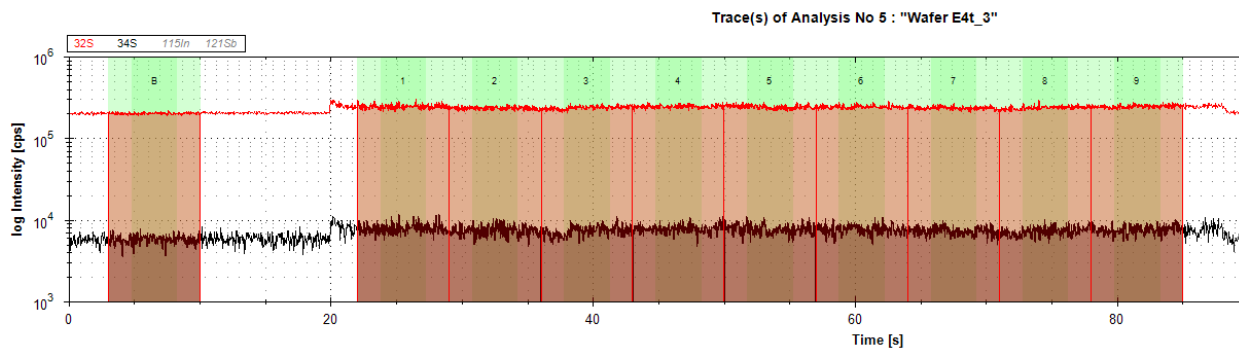


Figure 34: Time-scan of LA-ICP-MS analysis of Wafer E4t

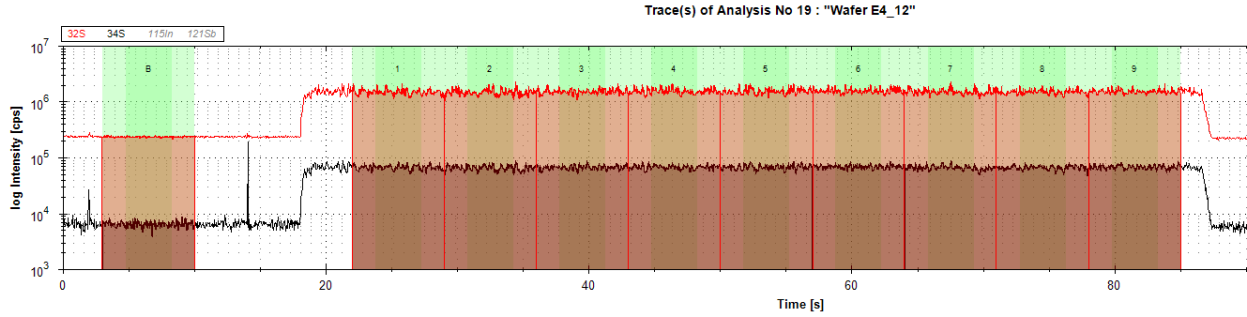


Figure 35: Time-scan of LA-ICP-MS analysis of Wafer E4

In Figure 35 time-scan of wafer E4 can be seen. Sulfur intensity gained for E4 is significantly higher than for E4t. This confirms results from liquid ICP-OES analysis. For results of wafer E4 analysis see Figure 36. A homogeneous sulfur distribution occurs in this wafer.

LOD derived for these analyses was 39 mg/kg (ppm).

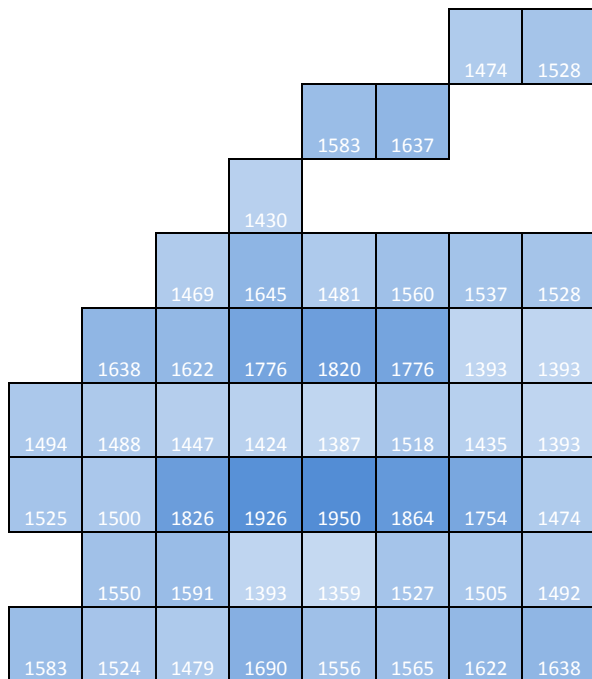


Figure 36: LA-ICP-MS measurement of E4 and E4t, [mg/kg] sulfur in solid sample

Average sulfur concentration in solid sample was 1567 ± 145 mg/kg (ppm) sulfur. This concentration is comparable to the one derived from liquid analysis, however it is a bit lower. The difference can maybe be related to the depth distribution of sulfur in the copper layer. For this depth profiles were measured with SIMS, see next chapter.

3.3.3. SIMS

Depth profiles of all wafers were analyzed by Silvia Larisegger and Florian Brenner. In this chapter results for E1, E4 and E4t, see Figure 37 to Figure 39, are shown. SIMS analyses of remaining wafers are shown in Appendix.

Wafers E1 and E1t provided almost no intensity, leading to the conclusion that wafers manufactured with these additives contain no sulfur. For E2, E2t, E3 and E3t more count could be detected, but since no possibility for sulfur quantification in a copper matrix was given, it cannot be said how much sulfur this is equal to. Trends show that sulfur concentration decreases with layer depth. This can also be said for wafer E4t. Those results confirm results gained from ICP-OES and LA-ICP-MS measurements.

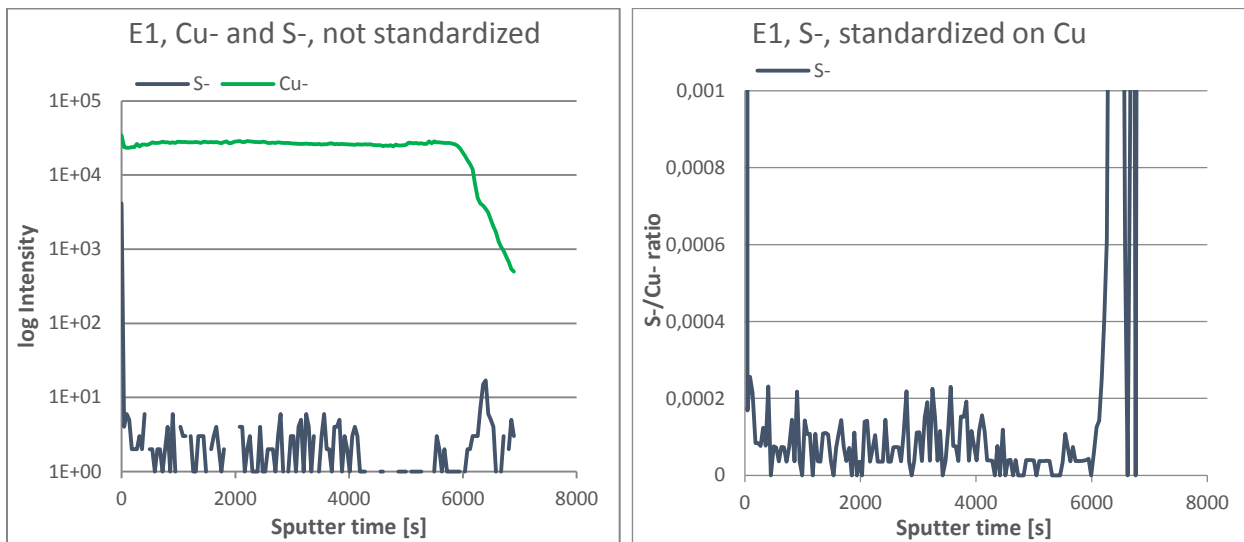


Figure 37: Wafer E1, S- and Cu- not standardized, S- standardized on Cu

In comparison to wafers E1, E2 and E3 signal intensity for sulfur is significantly higher in wafer E4, see Figure 38. An increase of sulfur signal with time can be observed.

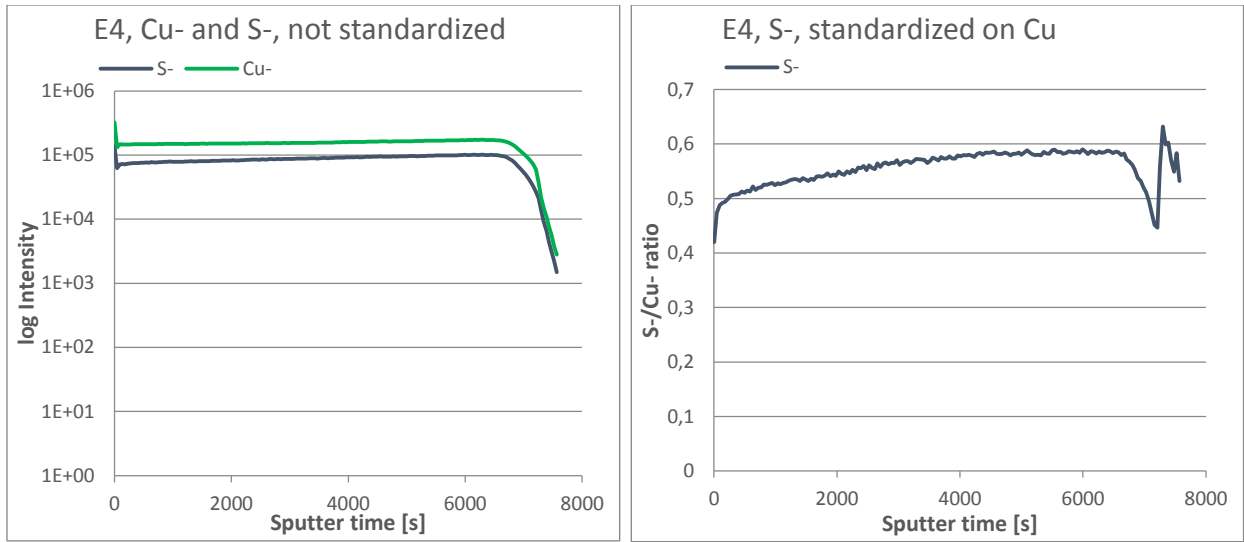


Figure 38: Wafer E4, S- and Cu- not standardized, S- standardized on Cu

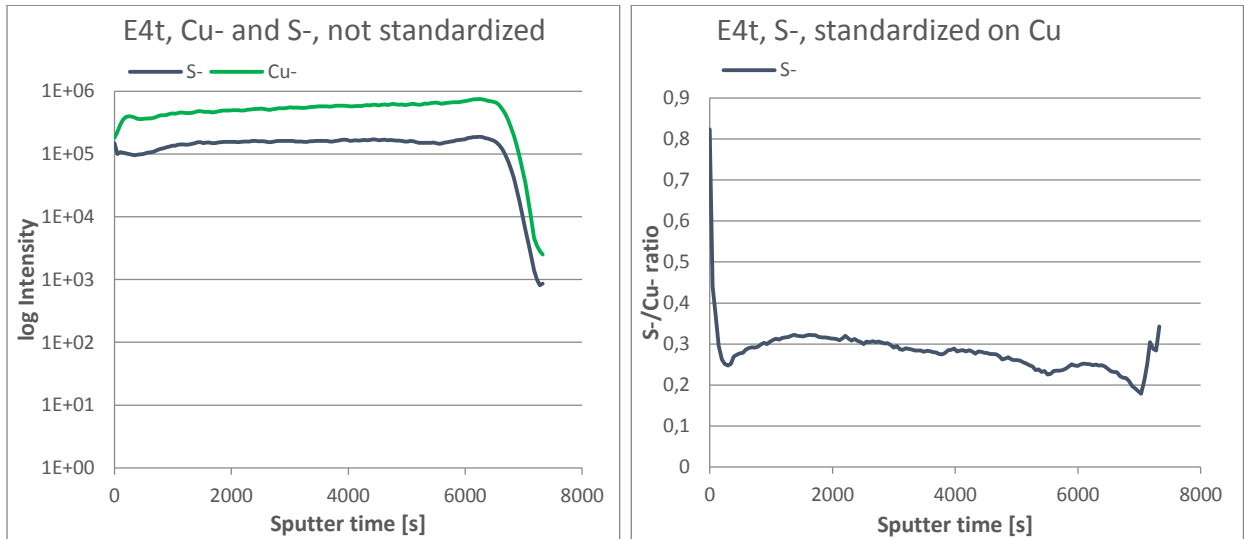


Figure 39: Wafer E4t, S- and Cu- not standardized, S- standardized on Cu

A reason for the concentration difference between liquid ICP-OES and solid sample LA-ICP-MS analysis can be seen in Figure 38. It can be observed that the sulfur concentration increases with layer depth. SIMS analysis of E4 is evidence to suggest that the concentration difference derives from non-entire layer ablation when using LA. Intensities measured for E4t were lower than for E4.

4. Conclusion and Outlook

Content of this work was to establish ICP-based methods for sulfur quantification in copper wafers. For that two different approaches were chosen. Direct analysis of the copper layers using Laser Ablation (LA) and quantification for digested liquid samples. Each approach should be conducted using ICP-MS and ICP-OES. Method development for sulfur analysis using ICP-based methods was successful.

With usage of a reactive cell when measuring liquid samples with ICP-MS spectral interferences of $^{16}\text{O}^{16}\text{O}$ could be avoided by detecting sulfur as $^{16}\text{O}^{32}\text{S}$ on $m/z=48$. Linear slopes could be gained for sulfur calibration, LODs down to $\sim 2 \mu\text{g/L}$ (ppb) were derived. However, this method can only be applied if the solution is ^{48}Ti -free to avoid interferences on $m/z=48$. Since the copper wafers analyzed in this work contained a WTi-barrier layer, which dissolved during sample digestion, this method could not be applied for sulfur quantification on the wafers.

Another method for liquid sample analysis was ICP-OES. Coupled with APEX E sensitivity sufficient for analysis of digested samples was derived. LODs down to $5 \mu\text{g/L}$ (ppb) were obtained. This method was successfully used for sulfur quantification in copper-layers of wafers.

LA coupling worked with both ICP-MS and ICP-OES, though significantly lower LOD was derived for LA-ICP-MS. Major advantage of using LA is that no sample preparation is necessary, reducing the risk of contaminations or dilution errors. For sulfur analysis a problem derives when using LA. Some of the tubing in the instrument contains sulfur, resulting in a sulfur background signal. The background could be decreased, but due to the tubing not eliminated, by purging the LA-ablation chamber for two hours. Because of purging the LA instrument, oxygen is removed and therefore spectral interferences from $^{16}\text{O}^{16}\text{O}$ do not occur on $m/z=32$. This method was successfully applied for sulfur quantification in copper wafers.

Comparison of the two different methods applied for sulfur quantification in copper wafers is shown in Table 17. Sulfur concentration above LOD could only be obtained for wafers E4 and E4t. For the other wafers, E1 to E3 and E1t to E3t, only information that could be derived was to say that the sulfur concentration is lower the LOD gained. LOD was then referenced to the amount of copper-layer digested. Concentration of sulfur in those solid wafers is lower than $\sim 10 \text{ mg/kg}$ (ppm).

Table 17: Comparison of sulfur concentration of applied analysis methods

| Instrument | Average [mg/kg] | Standard deviation [mg/kg] | RSD [%] |
|------------|-----------------|----------------------------|---------|
| E4 | | | |
| ICP-OES | 1820 | 129 | 7 |
| LA-ICP-MS | 1567 | 145 | 9 |
| E4t | | | |
| ICP-OES | 335 | 17 | 5 |

Comparison shows that resulting sulfur concentration average for E4 is higher from ICP-OES measurement than from LA-ICP-MS analysis. Inside the margin of error however, an overlap of concentrations occurs. Depth profiling with SIMS was used to see how sulfur is distributed in the copper layer, only quantification and no qualification was measured. Results show that sulfur concentration increases in depth. Since not all of the copper-layer is ablated during LA-ICP-MS measurement the concentration difference between these two methods can be explained through this. Homogeneous distribution of sulfur was detected with both methods.

A difference in material between wafers E4 and E4t compared to the other wafers could be observed. Wafers with high sulfur concentration appear to be more brittle. Between E4 and E4t a significant concentration difference occurs, leading to the assumption that sulfur evaporates during tempering process.

To determinate the difference of sulfur concentration for E4t the employment of an internal standard for LA-ICP-MS analysis of solid wafer samples is necessary.

For further experiments wafer E4 and E4t will be manufactured without the WTi-barrier layer. Analysis with ICP-MS will then be possible, allowing measurement of $^{16}\text{O}^{32}\text{S}$ without interference of ^{48}Ti on $m/z=48$.

References

- (n.d.). Retrieved from <http://em-1.stanford.edu/Schedule/ICP/abouticp.htm>.
- (n.d.). Retrieved from <http://upload.wikimedia.org/wikipedia/commons/3/3d/ICP-Brennerduese.png>.
- (n.d.). Retrieved from <http://www.icpms.com/pdf/ApexE-ESI.pdf>.
- Balcaen, L., Woods, G., Resano, M., & Vanhaecke, F. (2012). Accurate determination of S in organic matrices using isotope dilution ICP-MS/MS. *Journal of Analytical Atomic Spectrometry*.
- Bonta, M. (2013). *Elemental imaging using LA-ICP-MS on biological samples*. Vienna: TU Vienna.
- Fugger, M. (2014). *Dissertation*. Vienna: TU Vienna.
- Guillong, M., Latkoczy, C., Hun Seo, J., Günther, D., & Heinrich, C. (2008, October). Determination of sulfur in fluid inclusions by laser ablation ICP-MS. *Journal of Analytical Atomic Spectrometry*.
- Günther, D., & Hattendorf, B. (2005). Solid sample analysis using laser ablation inductively coupled plasma mass spectrometry. *Trends in Analytical Chemistry*, pp. Vol.24, No.3.
- Larisegger, S. (2014). *Dissertation*. Vienna: TU Vienna.
- Mason, P., Kaspers, K., & Bergen, M. v. (1999, May). Determination of sulfur isotope ratios and concentrations in water samples using ICP-MS incorporating hexapole ion optics. *Journal of Analytical Atomic Spectrometry*.
- Mokgalaka, N., & Gardea-Torresdey, J. (2006, November). Laser Ablation Inductively Coupled Plasma Mass Spectrometry: Principles and Applications. *Applied Spectroscopy Reviews*.
- Montaser, A. (1998). *Inductively Coupled Plasma Mass Spectrometry*. Wiley-VCH.
- Nischkauer, W. (2011). *Development of advanced methods for the determination of Platinum Group Elements in plant material*. Vienna: TU Vienna.

- Olesik, J. W. (1991, January). Elemental Analysis Using An Evaluation and Assessment of Remaining Problems. *Analytical Chemistry*, pp. 12-21.
- Pereira, J. S., Mello, P. A., Moraes, D. P., Duarte, F. A., Dressler, V. L., Knapp, G., & Flores, É. M. (2009). Chlorine and sulfur determination in extra-heavy crude oil by inductively coupled plasma optical emission spectrometry after microwave-induced combustion. *Spectrochimica Acta Part B*.
- Prohaska, T., Latkoczy, C., & Stingeder, G. (1999). Precise sulfur isotope ratio measurements in trace concentration of sulfur by inductively coupled plasma double focusing sector field mass spectrometry. *Journal of Analytical Atomic Spectrometry*.
- Robl, W., Melzl, M., Weidgans, B., Hofmann, R., & Stecher, M. (2008, August). Last Metal Copper metallization for Power Devices. *IEEE Transactions on Semiconductor Manufacturing*.
- Santelli, R. E., Oliveira, E. P., de Carvalho, M. d., Bezerra, M. a., & Freire, A. S. (2008). Total sulfur determination in gasoline, kerosene and diesel fuel using inductively coupled plasma optical emission spectrometry after direct sample introduction as detergent emulsions. *Spectrochimica Acte Part B*.
- Thomas, R. (2001, September). A Beginner's Guide to ICP-MS, Part V: The Ion Focusing System. *Spectroscopy*.
- Thomas, R. (2001, October). A Beginner's guide to ICP-MS, Part VI- The Mass Analyser. *Spectroscopy*.
- Thomas, R. (2002, February). A Beginner's Guide to ICP-MS, Part IX - Mass Analyzers: Collision/Reaction Cell Technology. *Spectroscopy*.
- Thomas, R. (2002, April). A Beginner's Guide to ICP-MS, Part X- Detectors. *Spectroscopy*.

List of figures

| | |
|---|----|
| Figure 1: Set-up of a LA system, coupled with an ICP-MS | 15 |
| Figure 2: ICP Torch | 18 |
| Figure 3: Vacuum interface, ICP-MS | 21 |
| Figure 4: Quadrupole mass separation device | 23 |
| Figure 5: Collision cell, empty | 26 |
| Figure 6: Collision cell, sulfur ions enter into the cell..... | 27 |
| Figure 7: Collision cell, sulfur ions and O ₂ as reactive gas | 28 |
| Figure 8: Collision cell, analyte, reaction gas and new formed compound | 28 |
| Figure 9: Half copper wafer | 31 |
| Figure 10: Quarter copper wafer | 32 |
| Figure 11: Quarter copper wafer, scratched | 32 |
| Figure 12: ThermoFisher Scientific iCAP Q; ICP-MS instrumentation for performed experiments... | 33 |
| Figure 13: New Wave 213 ESI, Laser instrumentation used for performed experiments | 34 |
| Figure 14: Ablation pattern | 35 |
| Figure 15: Time-scan, LA-ICP-MS measurement, Blank- and region areas | 36 |
| Figure 16: ThermoFisher Scientific iCAP 6000; ICP-OES instrumentation for performed experiments | 36 |
| Figure 17: ION-TOF GmbH, TOF-SIMS 5 | 41 |
| Figure 18: ICP-MS measurement, Comparison calibration standard- vs CCT-mode..... | 42 |
| Figure 19: ICP-OES-measurement, coupled with APEX E, first calibration | 44 |
| Figure 20: LA-ICP-OES measurement, Distribution of sulfur and antimony in pellets, prepared with 10 resp. 30 spheres, Numbers see Table 18 and Table 19 | 46 |
| Figure 21: LA- ICP-OES measurement, Distribution and linearity of sulfur and antimony in pellet with composition 4 | 47 |
| Figure 22: LA-ICP-OES measurement, calibration with pellets, Numbers see Table 20 | 48 |
| Figure 23: LA-ICP-MS measurement, laser-mode, calibration with pellets, without standard 500 ppm (outlier), for Numbers see Table 21 | 49 |
| Figure 24: Time-scan of LA-ICP-MS analysis of pellet with 100 ppm sulfur concentration | 50 |
| Figure 25: Time-scan of LA-ICP-MS analysis of pellet with 500 ppm sulfur concentration | 50 |
| Figure 26: Time-scan of LA-ICP-MS analysis of pellet with 750 ppm sulfur concentration | 50 |

| | |
|--|----|
| Figure 27: Wafer E1 and E4, comparison | 51 |
| Figure 28: Color scale used in chapter 3..... | 52 |
| Figure 29: ICP-MS with reaction cell analysis, Wafer E1 and E2, [mg/kg] sulfur in solid..... | 52 |
| Figure 30: ICP-MS with reaction cell analysis, Wafer E3 and E4, [mg/kg] sulfur in solid..... | 53 |
| Figure 31: ICP-OES analysis of wafer E1, LOD for solid sample [mg/kg]..... | 54 |
| Figure 32: ICP-OES analysis of E4, [mg/kg] sulfur in solid sample..... | 57 |
| Figure 33: Time-scan of LA-ICP-MS analysis of Wafer E1..... | 58 |
| Figure 34: Time-scan of LA-ICP-MS analysis of Wafer E4t..... | 58 |
| Figure 35: Time-scan of LA-ICP-MS analysis of Wafer E4..... | 59 |
| Figure 36: LA-ICP-MS measurement of E4 and E4t, [mg/kg] sulfur in solid sample | 59 |
| Figure 37: Wafer E1, S- and Cu- not standardized, S- standardized on Cu..... | 60 |
| Figure 38: Wafer E4, S- and Cu- not standardized, S- standardized on Cu..... | 61 |
| Figure 39: Wafer E4t, S- and Cu- not standardized, S- standardized on Cu..... | 61 |
| Figure 40: Wafer E1t, S- and Cu- not standardized, S- standardized on Cu..... | 71 |
| Figure 41: Wafer E2, S- and Cu- not standardized, S- standardized on Cu..... | 71 |
| Figure 42: Wafer E2t, S- and Cu- not standardized, S- standardized on Cu..... | 72 |
| Figure 43: Wafer E3, S- and Cu- not standardized, S- standardized on Cu..... | 72 |
| Figure 44: Wafer E3t, S- and Cu- not standardized, S- standardized on Cu..... | 73 |

List of tables

| | |
|---|----|
| Table 1: Spectral interferences at m/z 32 and 34 | 25 |
| Table 2: Sample identification | 31 |
| Table 3: Measurement parameters of iCAP Q, ICP-MS | 34 |
| Table 4: Laser parameters | 35 |
| Table 5: OES measurement parameters | 37 |
| Table 6: Pellet composition, rounded, all contain 100 ppm sulfur | 38 |
| Table 7: Chemicals used for copper wafer digestion | 39 |
| Table 8: Chemicals used for calibration standards..... | 40 |
| Table 9: Chemicals used for matrix matched calibration | 40 |
| Table 10: LA-ICP_MS measurement, Optimization of laser beam diameter for ³⁴ S and ¹²³ Sb, Region Area | 45 |
| Table 11: LOD's for calibrations obtained with LA-ICP-OES and LA-ICP-MS | 51 |
| Table 12: ICP-OES analysis of Wafer E1t..... | 55 |
| Table 13: ICP-OES analysis of Wafer E2 and E2t..... | 55 |
| Table 14: ICP-OES analysis of Wafer E3..... | 56 |
| Table 15: ICP-OES analysis of Wafer E4t, [mg/kg] sulfur in solid sample | 57 |
| Table 16: ICP-OES measurements, Sulfur concentration average of Wafers E4 and E4t | 57 |
| Table 17: Comparison of sulfur concentration of applied analysis methods | 63 |
| Table 18: LA- ICP-OES measurement, Distribution of sulfur and antimony in pellets, prepared with 10 spheres | 69 |
| Table 19: LA- ICP-OES measurement, Distribuion of sulfur and antimony in pellets, prepared with 30 spheres | 69 |
| Table 20: LA-ICP-OES measurement, calibration with pellets | 70 |
| Table 21: LA-ICP-MS measurement, laser-mode, calibration with pellets | 70 |

Appendix

Table 18: LA- ICP-OES measurement, Distribution of sulfur and antimony in pellets, prepared with 10 spheres

| Pellet | Average [cts/s] | Standard deviation [cts/s] | RSD [%] |
|---------------------|-----------------|----------------------------|---------|
| S, 180,7 nm | | | |
| 10 Spheres_1 | 14,4 | 1,76 | 12,3 |
| 10 Spheres_2 | 10,2 | 1,61 | 15,8 |
| 10 Spheres_3 | 17,8 | 2,84 | 16,0 |
| 10 Spheres_4 | 21,3 | 1,85 | 8,70 |
| 10 Spheres_5 | 21,2 | 1,60 | 7,54 |
| 10 Spheres_6 | 14,2 | 1,57 | 11,1 |
| 10 Spheres_7 | 16,6 | 1,87 | 11,3 |
| Sb, 206,8 nm | | | |
| 10 Spheres_1 | 94,6 | 12,65 | 13,4 |
| 10 Spheres_2 | 66,2 | 14,95 | 22,6 |
| 10 Spheres_3 | 130,0 | 22,35 | 17,2 |
| 10 Spheres_4 | 144,8 | 19,79 | 13,7 |
| 10 Spheres_5 | 151,4 | 14,10 | 9,31 |
| 10 Spheres_6 | 101,4 | 15,63 | 15,4 |
| 10 Spheres_7 | 124,9 | 19,88 | 15,9 |

Table 19: LA- ICP-OES measurement, Distributuion of sulfur and antimony in pellets, prepared with 30 spheres

| Pellet | Average [cts/s] | Standard deviation [cts/s] | RSD [%] |
|---------------------|-----------------|----------------------------|---------|
| S, 180,7 nm | | | |
| 30 Spheres_1 | 17,7 | 6,60 | 37,4 |
| 30 Spheres_2 | 8,6 | 1,27 | 14,7 |
| 30 Spheres_3 | 13,2 | 1,91 | 14,5 |
| 30 Spheres_4 | 18,2 | 2,64 | 14,5 |
| 30 Spheres_5 | 21,7 | 3,09 | 14,2 |
| 30 Spheres_6 | 18,4 | 3,23 | 17,5 |
| 30 Spheres_7 | 13,9 | 2,96 | 21,3 |
| Sb, 206,8 nm | | | |
| 30 Spheres_1 | 131,6 | 49,81 | 37,8 |
| 30 Spheres_2 | 65,6 | 9,47 | 14,5 |
| 30 Spheres_3 | 98,0 | 8,93 | 9,11 |
| 30 Spheres_4 | 127,0 | 26,40 | 20,8 |
| 30 Spheres_5 | 144,1 | 23,64 | 16,4 |
| 30 Spheres_6 | 124,2 | 23,96 | 19,3 |
| 30 Spheres_7 | 91,0 | 13,74 | 15,1 |

Table 20: LA-ICP-OES measurement, calibration with pellets

| Ppm sulfur in pellet | Average [Cts/s] | Standard deviation [Cts/s] | RSD [%] |
|----------------------|-----------------|----------------------------|---------|
| S, 180,7 nm | | | |
| 0 | 1,02 | 0,59 | 58 |
| 50 | 1,58 | 0,35 | 22 |
| 100 | 1,75 | 0,22 | 12 |
| 250 | 3,15 | 0,80 | 25 |
| 500 | 5,55 | 1,49 | 27 |
| 750 | 7,90 | 0,74 | 9 |
| Sb, 206,8 nm | | | |
| 0 | 0,04 | 0,531 | 1382 |
| 50 | 2,18 | 0,900 | 41 |
| 100 | 4,41 | 0,819 | 19 |
| 250 | 12,49 | 4,414 | 35 |
| 500 | 23,73 | 5,834 | 25 |
| 750 | 33,88 | 2,483 | 7 |

Table 21: LA-ICP-MS measurement, laser-mode, calibration with pellets

| Ppm sulfur in pellet | Average [cts] | Standard deviation [cts] | RSD [%] |
|-------------------------|---------------|--------------------------|---------|
| ³²S | | | |
| 0 | 196739 | 24438 | 12 |
| 50 | 360507 | 19949 | 6 |
| 100 | 475041 | 55813 | 12 |
| 250 | 1229310 | 127021 | 10 |
| 500 | 1797797 | 84539 | 5 |
| 750 | 3206300 | 253195 | 8 |
| ³⁴S | | | |
| 0 | 10595 | 1468 | 14 |
| 50 | 19042 | 2071 | 11 |
| 100 | 24128 | 2779 | 12 |
| 250 | 60347 | 6736 | 11 |
| 500 | 88672 | 4340 | 5 |
| 750 | 154663 | 8772 | 6 |
| ¹²¹Sb | | | |
| 0 | 765765 | 56202 | 7 |
| 50 | 6914261 | 822133 | 12 |
| 100 | 12000434 | 2346892,8 | 20 |
| 250 | 40047656 | 4675840 | 12 |
| 500 | 57198026 | 2072834 | 4 |
| 750 | 106108237 | 9489704 | 9 |

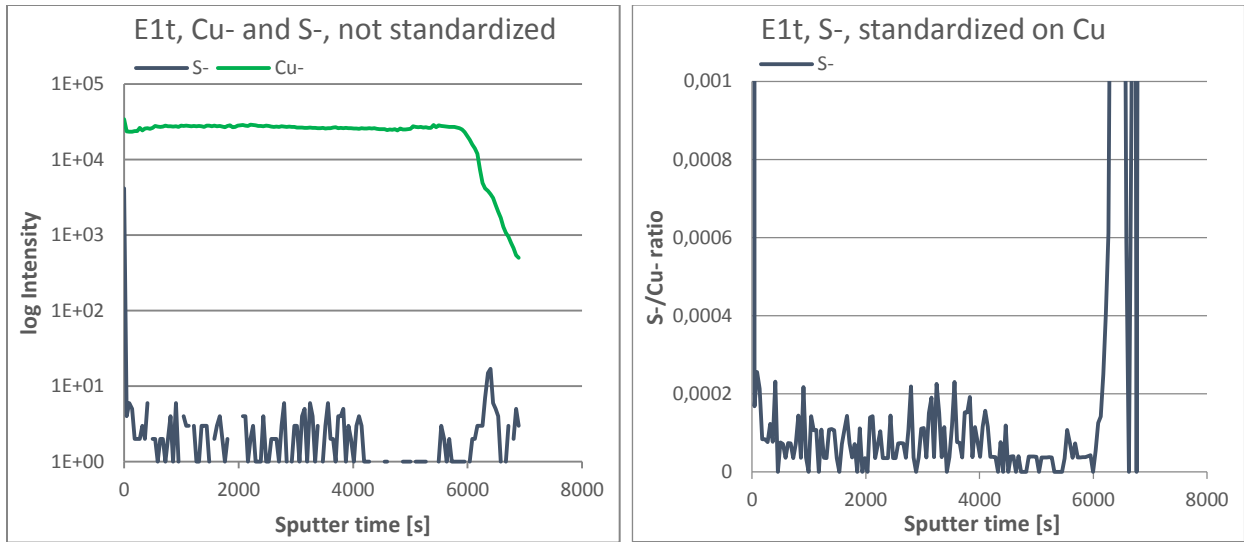


Figure 40: Wafer E1t, S- and Cu- not standardized, S- standardized on Cu

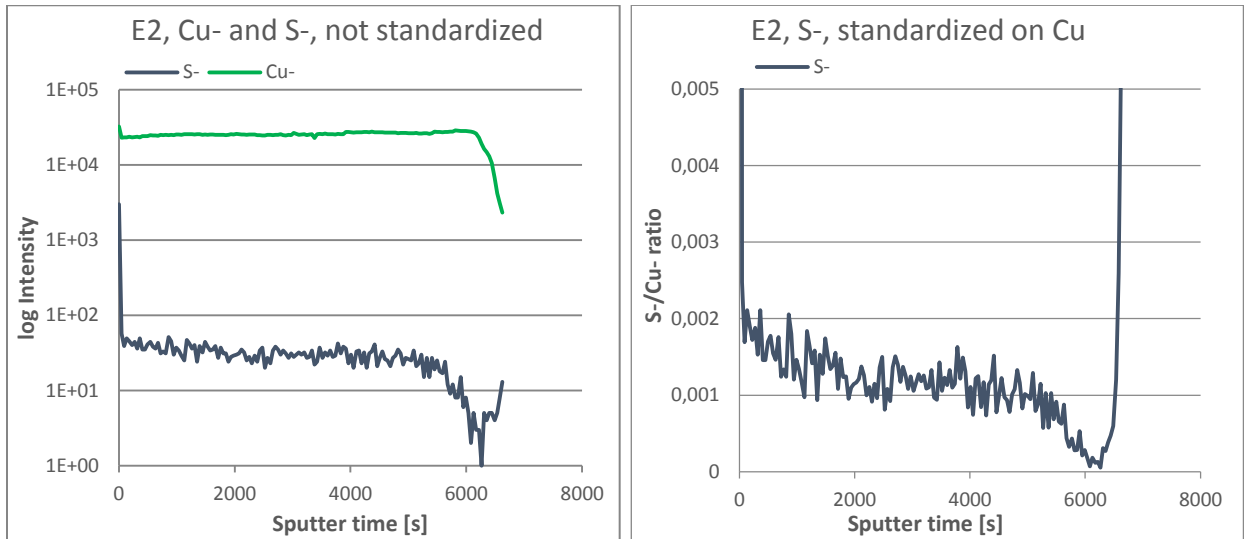


Figure 41: Wafer E2, S- and Cu- not standardized, S- standardized on Cu

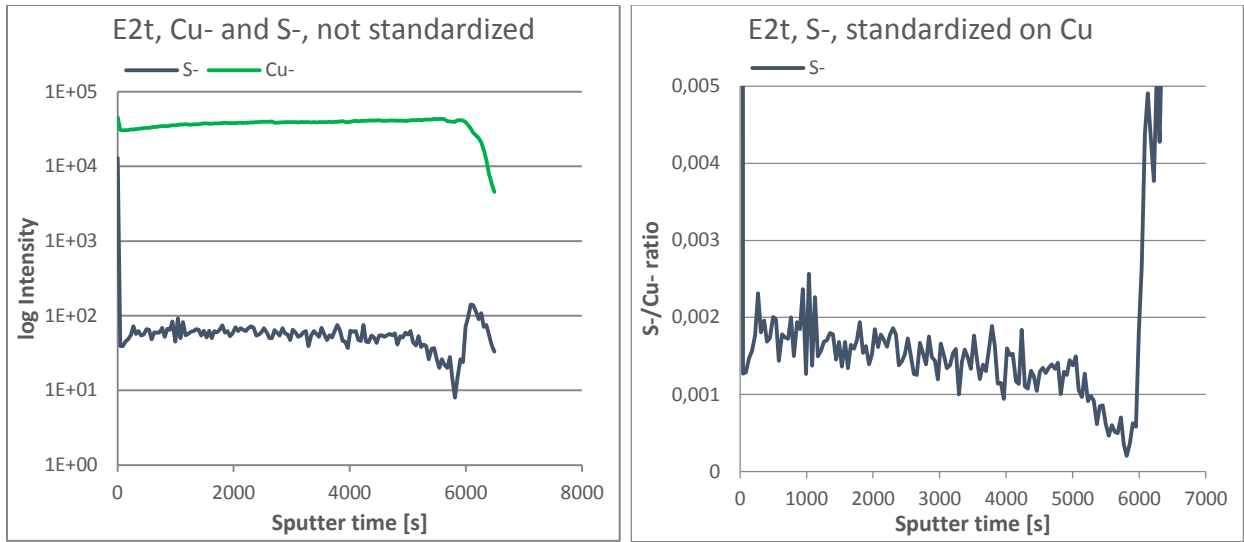


Figure 42: Wafer E2t, S- and Cu- not standardized, S- standardized on Cu

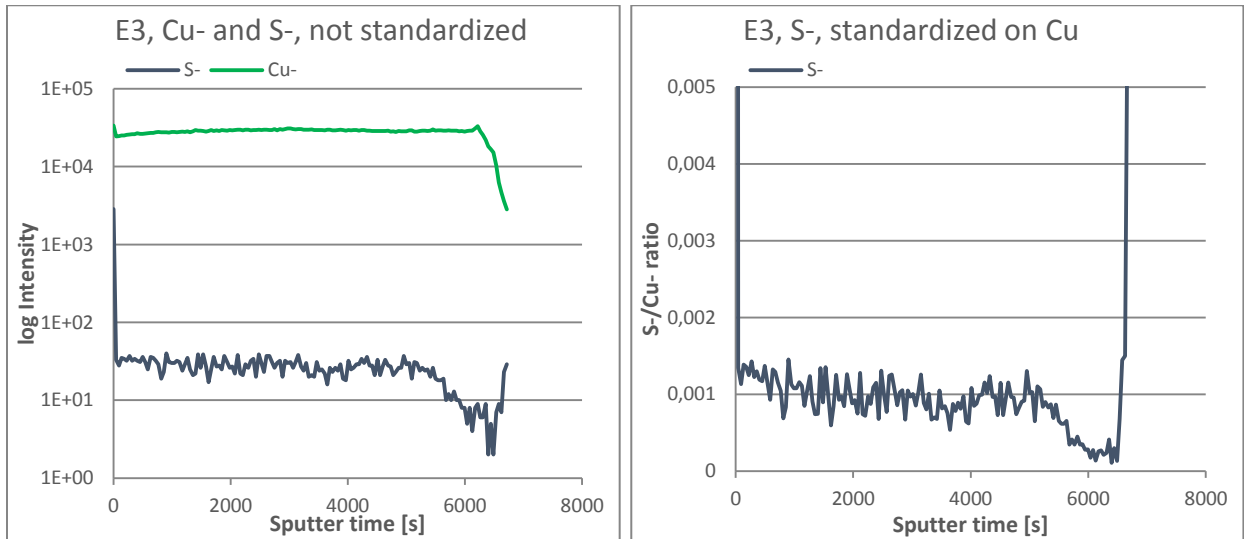


Figure 43: Wafer E3, S- and Cu- not standardized, S- standardized on Cu

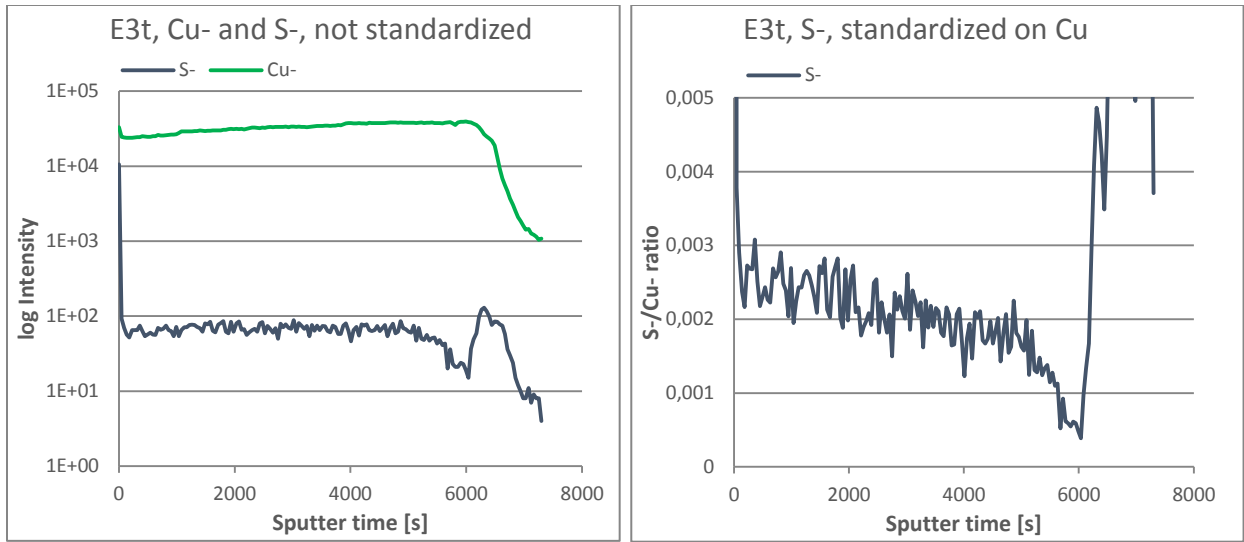


Figure 44: Wafer E3t, S- and Cu- not standardized, S- standardized on Cu